
Perfectly-Matched Metamaterials

Shrey Thakkar, Jorge Ruiz-Garcia and Anthony Grbic

Radiation Laboratory, Department of EECS,
University of Michigan, USA
agrbic@umich.edu

Collaborators:

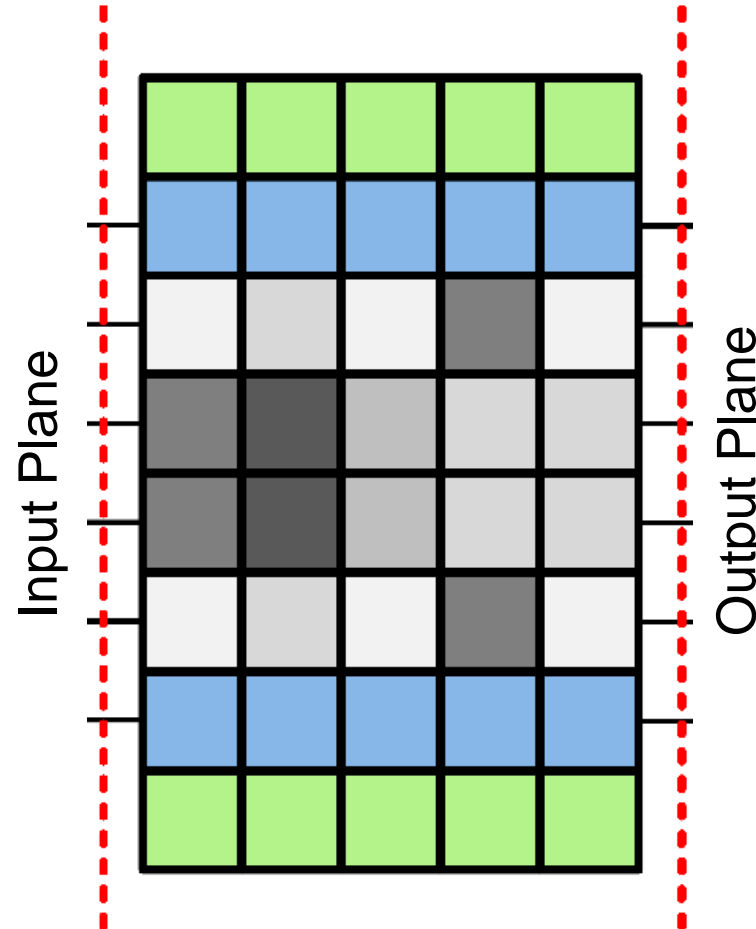
Dr. Luke Szymanski, MIT Lincoln Laboratory, Lexington, MA, USA
Dr. Gurkan Gok, RTX Technology Research Center, East Hartford, USA



AFOSR Grant FA9550-24-1-0098

The metamaterial playground

- MIMO metamaterials map a set of inputs to a set of outputs.
- The space between the input and output planes is the metamaterial playground: an anisotropic inhomogeneous medium.



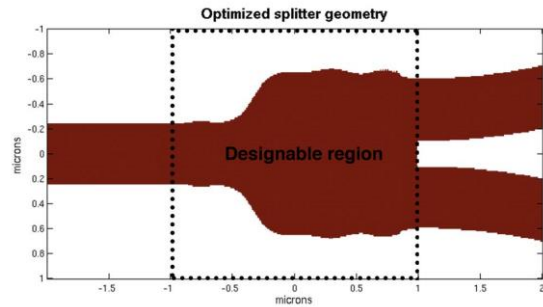
[1] B. B. Tierney and A. Grbic, *IEEE Trans. on Antennas and Propagation*, vol. 67, no. 2, pp. 998 – 1009, Feb. 2019.

[2] B. B. Tierney and A. Grbic, *IEEE Trans. on Antennas and Propagation*, vol. 66, no. 9, pp. 4844 – 4853, Sept. 2018.

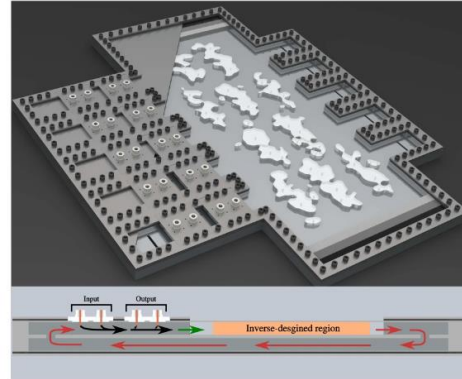
Inverse design in electromagnetics

Full-wave Methods

[1]

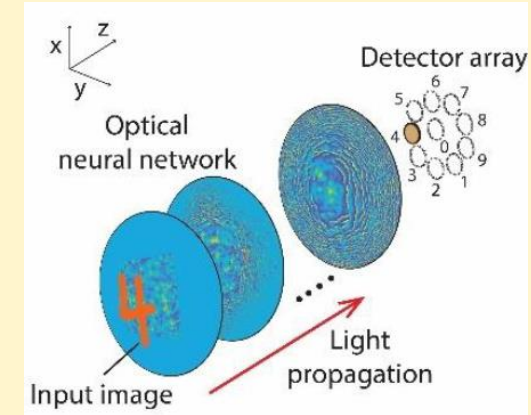


[2]



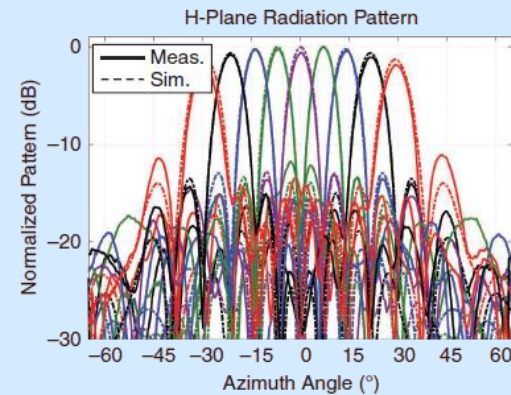
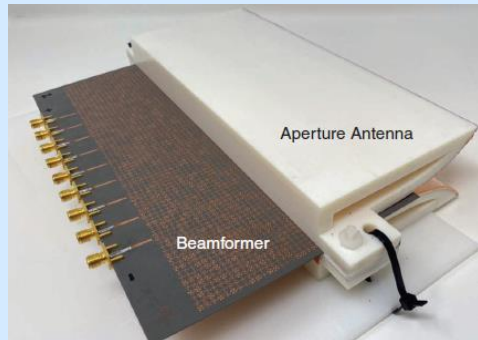
Scalar Diffraction Theory

[3]



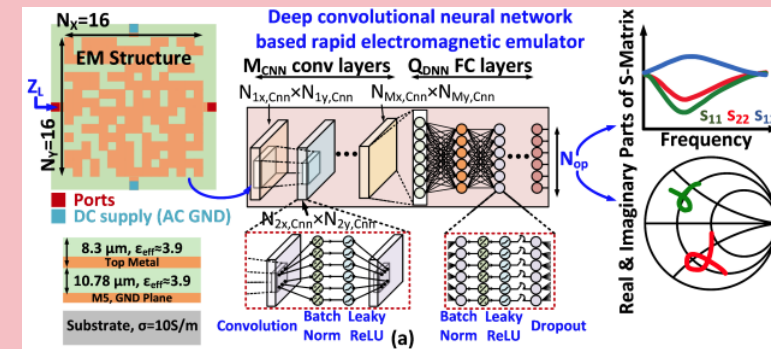
Surrogate Models

[4]



Neural Networks

[5]



[1] C.M. Lalau-Keraly, S. Bhargava, O.D. Miller, E. Yablonovitch, *Optics Express*, vol. 21, no. pp. 18, 21693-21701, 2013

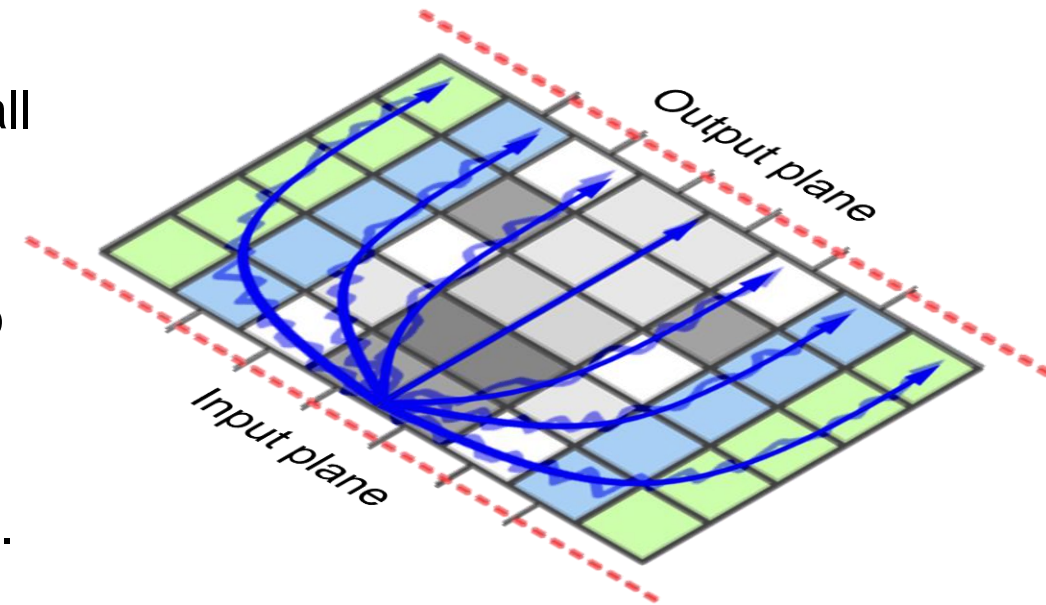
[2] M. Camacho, B. Edwards, and N. Engheta, *Nat Commun*, vol. 12, no. 1, p. 1466, Mar. 2021

[3] A. Backer, *Optics Express*, Vol. 27, Issue 21, pp. 30308-30331, (2019)

[4] L. Szymanski, G. Gok, and A. Grbic, *IEEE Antennas Propag. Mag.*, vol. 64, no. 4, pp. 63–72, Aug. 2022.

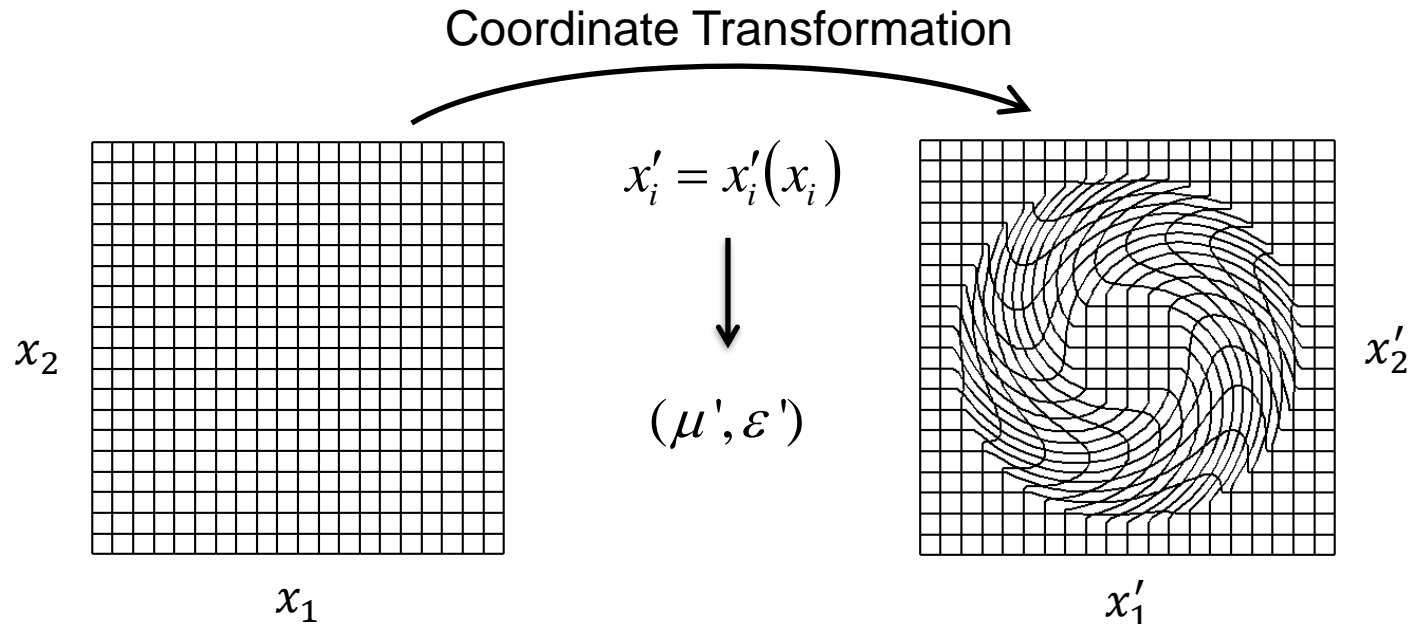
[5] Z. Liu et al, *IEEE Microw. Wireless Compon. Lett.*, vol. 32, no. 6, pp. 724 - 727, Jun. 2022.

- Can an inhomogeneous, anisotropic metamaterial be designed whose constitutive unit cells are impedance matched to each other and to the surrounding space for all excitations/ illuminations?
- Such a metamaterial's performance would rely on refractive effects rather than intercell or bulk reflections to perform a prescribed function.
- If frequency dispersion could also be controlled, these metamaterials could provide true time-delay performance.



Transformation optics

- A desired field distribution is derived from an initial one through a coordinate transformation.
- The form invariance of Maxwell's equations under different coordinate transformations is then exploited to calculate the spatial distribution of material parameters (permittivity and permeability) required.
- Finding the coordinate transformation that yields the field of interest is not always intuitive or straightforward.
- Truncating the domains can also lead to impedance mismatches.



[1] J. B. Pendry, D. Schurig, and D. R. Smith, "Controlling electromagnetic fields," *Science*, vol. 312, pp. 1780-1782, 2006.

[2] U. Leonhardt, "Optical conformal mapping," *Science*, vol. 312, pp. 1777-1780, 2006.

How do we extend transformation optics to allow MIMO functionality?

Our metamaterial canvas



- 2D Medium is discretized into unit cells much smaller than the guided wavelength.

The following polarization is assumed:

- Electric field is out of plane. It is in the z direction: E_z
- Magnetic field is in plane. It is in the x and y directions: H_x, H_y

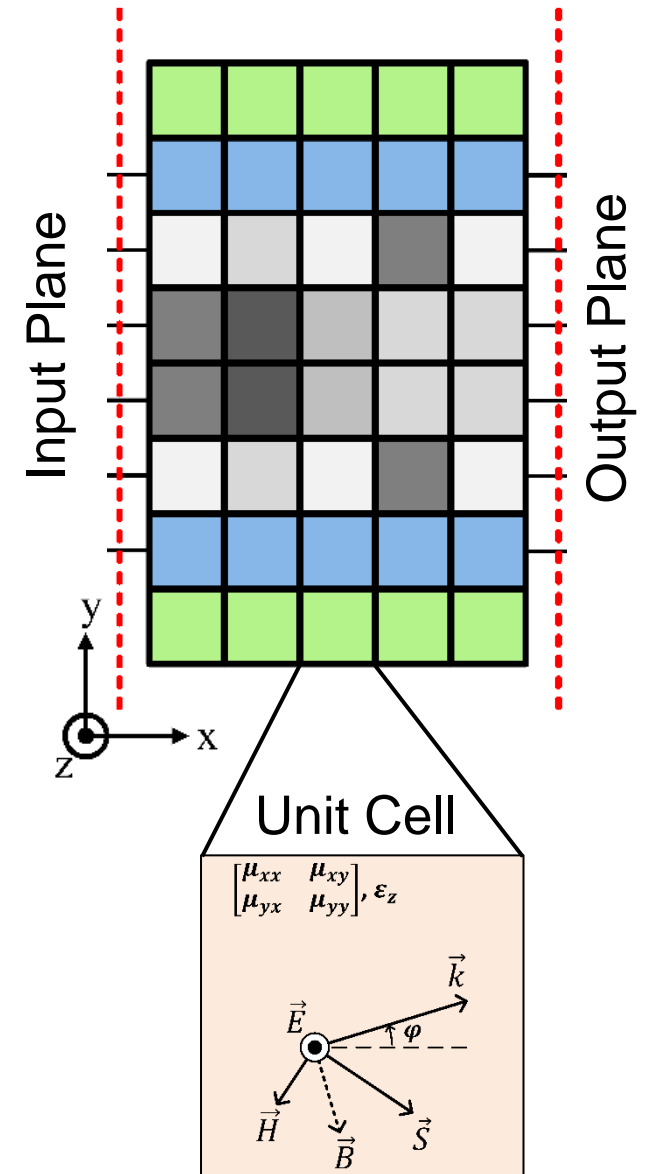
Relative material parameters

Permeability tensor

$$\bar{\bar{\mu}} = \begin{bmatrix} \mu_{xx} & \mu_{xy} \\ \mu_{yx} & \mu_{yy} \end{bmatrix}$$

Permittivity scalar

$$\epsilon = \epsilon_z$$



Maxwell's equations for time-harmonic plane waves

Relevant material parameters

$$\bar{\bar{\mu}} = \begin{bmatrix} \mu_{xx} & \mu_{xy} \\ \mu_{yx} & \mu_{yy} \end{bmatrix} \quad \varepsilon = \varepsilon_z$$

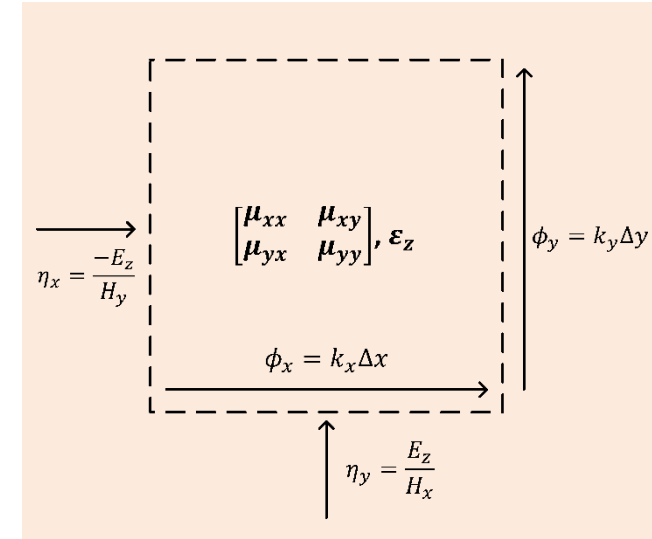
Maxwell's time-harmonic equations for plane waves:

Faraday's law

$$-j\vec{k} \times \vec{E} = -j\omega\bar{\bar{\mu}}\mu_o\vec{H} \quad (1)$$

Ampere's law

$$-j\vec{k} \times \vec{H} = -j\omega\varepsilon_z\varepsilon_o\vec{E} \quad (2)$$



Recast the two equations,

$$\begin{bmatrix} \bar{k}_y \\ \bar{k}_x \end{bmatrix} = \begin{bmatrix} \mu_{xx} & -\mu_{xy} \\ -\mu_{yx} & \mu_{yy} \end{bmatrix} \begin{bmatrix} \bar{\eta}_y^{-1} \\ \bar{\eta}_x^{-1} \end{bmatrix} \quad (3)$$

$$\varepsilon_z = \begin{bmatrix} \bar{k}_x & \bar{k}_y \end{bmatrix} \begin{bmatrix} \bar{\eta}_x^{-1} \\ \bar{\eta}_y^{-1} \end{bmatrix} \quad (4)$$

Normalized wave impedances

$$\bar{\eta}_x = -\frac{1}{\eta_o} \frac{E_z}{H_y}, \quad \bar{\eta}_y = \frac{1}{\eta_o} \frac{E_z}{H_x} \quad (5)$$

Normalized wave numbers

$$\bar{k}_x = \frac{k_x}{k_o}, \quad \bar{k}_y = \frac{k_y}{k_o} \quad (6)$$

Recasting Maxwell's equations

Faraday's Law

$$\begin{bmatrix} \bar{k}_y \\ \bar{k}_x \end{bmatrix} = \begin{bmatrix} \mu_{xx} & -\mu_{xy} \\ -\mu_{yx} & \mu_{yy} \end{bmatrix} \begin{bmatrix} 1/\bar{\eta}_y \\ 1/\bar{\eta}_x \end{bmatrix} \quad (4)$$

Ampere's Law

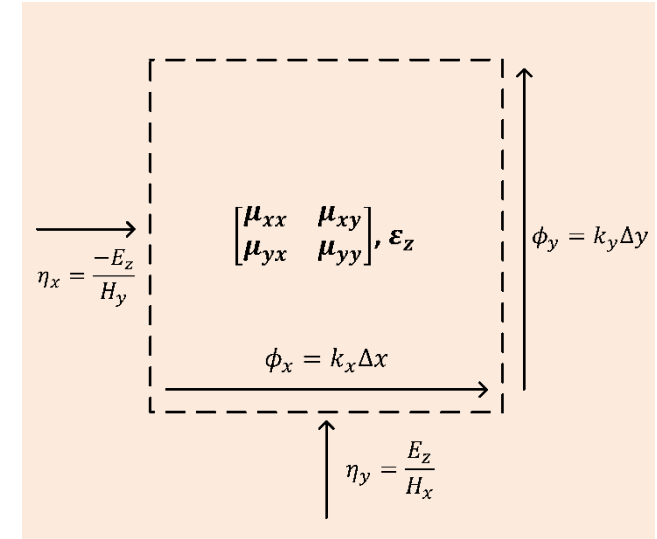
$$\varepsilon_z = \begin{bmatrix} \bar{k}_x & \bar{k}_y \end{bmatrix} \begin{bmatrix} 1/\bar{\eta}_x \\ 1/\bar{\eta}_y \end{bmatrix} \quad (5)$$

If the permeability tensor is reciprocal ($\mu_{xy} = \mu_{yx}$), Faraday's law can be rewritten as,

$$\begin{bmatrix} \bar{k}_x \\ \bar{k}_y \end{bmatrix} = |\bar{\mu}| \begin{bmatrix} \mu_{xx} & \mu_{xy} \\ \mu_{xy} & \mu_{yy} \end{bmatrix}^{-1} \begin{bmatrix} 1/\bar{\eta}_x \\ 1/\bar{\eta}_y \end{bmatrix} \quad (6)$$

Rearranging Faraday's Law (6) yields,

$$\frac{1}{|\bar{\mu}|} \left(\begin{bmatrix} \mu_{xx} & \mu_{xy} \\ \mu_{xy} & \mu_{yy} \end{bmatrix} \begin{bmatrix} \bar{k}_x \\ \bar{k}_y \end{bmatrix} \right) = \begin{bmatrix} 1/\bar{\eta}_x \\ 1/\bar{\eta}_y \end{bmatrix} \quad (7)$$



Dispersion equation

Faraday's Law

$$\frac{1}{|\bar{\mu}|} \begin{pmatrix} \mu_{xx} & \mu_{xy} \\ \mu_{xy} & \mu_{yy} \end{pmatrix} \begin{bmatrix} \bar{k}_x \\ \bar{k}_y \end{bmatrix} = \begin{bmatrix} 1/\bar{\eta}_x \\ 1/\bar{\eta}_y \end{bmatrix} \quad (7)$$

Ampere's Law

$$\varepsilon_z = [\bar{k}_x \quad \bar{k}_y] \begin{bmatrix} 1/\bar{\eta}_x \\ 1/\bar{\eta}_y \end{bmatrix} \quad (5)$$

Multiply both sides of Faraday's Law by vector $[\bar{k}_x \quad \bar{k}_y]$

$$\frac{[\bar{k}_x \quad \bar{k}_y]}{|\bar{\mu}|} \begin{pmatrix} \mu_{xx} & \mu_{xy} \\ \mu_{xy} & \mu_{yy} \end{pmatrix} \begin{bmatrix} \bar{k}_x \\ \bar{k}_y \end{bmatrix} = [\bar{k}_x \quad \bar{k}_y] \begin{bmatrix} 1/\bar{\eta}_x \\ 1/\bar{\eta}_y \end{bmatrix} \quad (8)$$

$$\frac{[\bar{k}_x \quad \bar{k}_y]}{|\bar{\mu}|} \begin{pmatrix} \mu_{xx} & \mu_{xy} \\ \mu_{xy} & \mu_{yy} \end{pmatrix} \begin{bmatrix} \bar{k}_x \\ \bar{k}_y \end{bmatrix} = \varepsilon_z \quad (8)$$

Expanding out this matrix equation, we obtain the dispersion equation for the magnetically anisotropic, homogeneous medium,

$$\bar{k}_x^2 \frac{\mu_{xx}}{|\bar{\mu}|} + 2\bar{k}_x \bar{k}_y \frac{\mu_{xy}}{|\bar{\mu}|} + \bar{k}_y^2 \frac{\mu_{yy}}{|\bar{\mu}|} = \varepsilon_z. \quad (9)$$

A rotated ellipse.

Relating wave impedance to tangential wavenumber

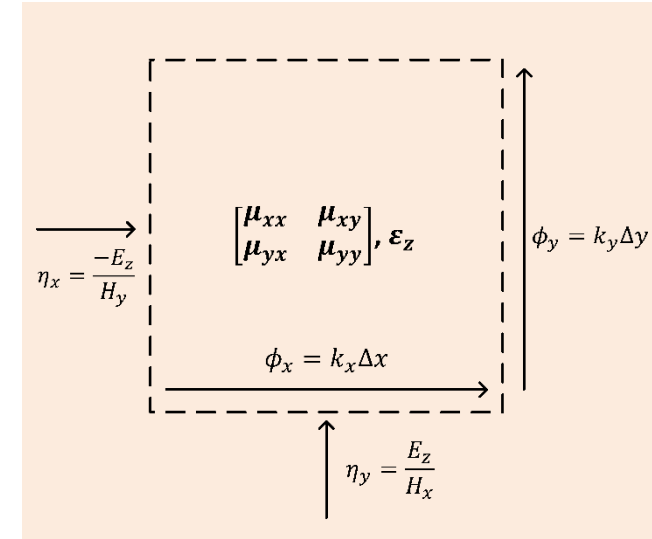
From the dispersion equation and Faraday's law, one can derive an equation relating wave impedance and tangential wavenumber,

$$\frac{1}{\bar{\eta}_x^2} = \frac{\mu_{xx}\epsilon_z}{|\bar{\mu}|} - \frac{(\bar{k}_y)^2}{|\bar{\mu}|}, (10a)$$

which can be rewritten as follows,

$$\frac{\left(\frac{1}{\bar{\eta}_x}\right)^2}{\frac{\mu_{xx}\epsilon_z}{|\bar{\mu}|}} + \frac{(\bar{k}_y)^2}{\mu_{xx}\epsilon_z} = 1. (10b)$$

- The wave impedance in the x direction, $\bar{\eta}_x$, and the wavenumber in the y direction, \bar{k}_y , are related in the magnetically anisotropic medium.
- The determinant of the permeability tensor ($|\bar{\mu}|$) and the refractive index ($\mu_{xx}\epsilon_z$) dictate the variation of the wave impedance $\bar{\eta}_x$ with the wavenumber \bar{k}_y .



Perfect matching at an interface

The half spaces are perfectly impedance-matched when their wave impedances $(\bar{\eta}_{x1}, \bar{\eta}_{x2})$ are equal for all angles of incidence (all \bar{k}_y values).

The wave impedances $\bar{\eta}_{x1}$ and $\bar{\eta}_{x2}$,

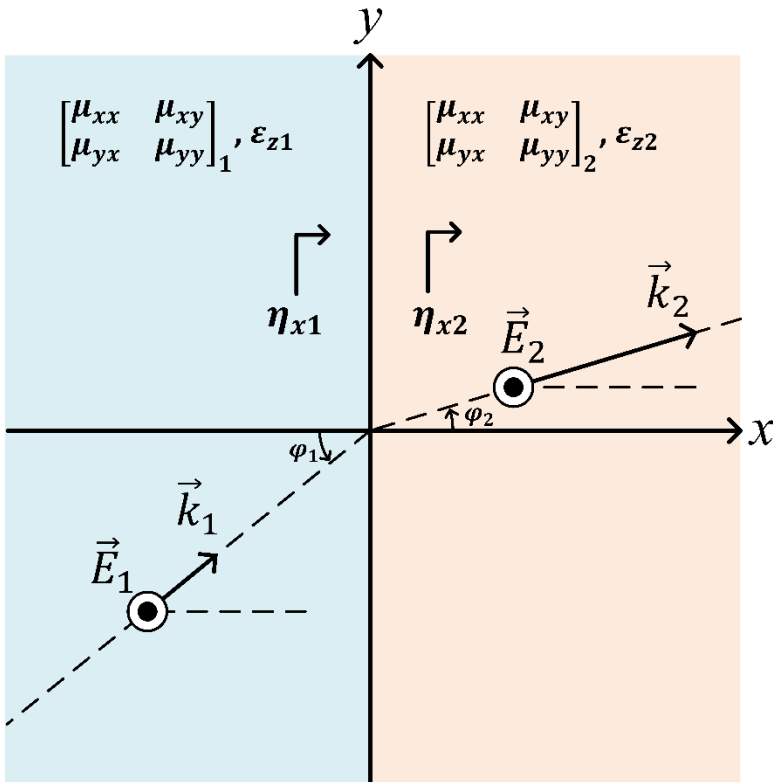
$$\left(\frac{1}{\bar{\eta}_{x1}}\right)^2 = \frac{\mu_{xx1}\varepsilon_{z1}}{|\bar{\mu}|_1} - \frac{(\bar{k}_y)^2}{|\bar{\mu}|_1} \quad \left(\frac{1}{\bar{\eta}_{x2}}\right)^2 = \frac{\mu_{xx2}\varepsilon_{z2}}{|\bar{\mu}|_2} - \frac{(\bar{k}_y)^2}{|\bar{\mu}|_2}$$

are matched only if the determinants of the permeability tensors for both media are equal and their normal refractive indices are equal,

Conditions for Perfect Matching

$$|\bar{\mu}|_1 = |\bar{\mu}|_2 = \Delta, \quad (11)$$

$$(\mu_{xx}\varepsilon_z)_1 = (\mu_{xx}\varepsilon_z)_2 = n_{yy}^2 \quad (12)$$



Material properties

Given,

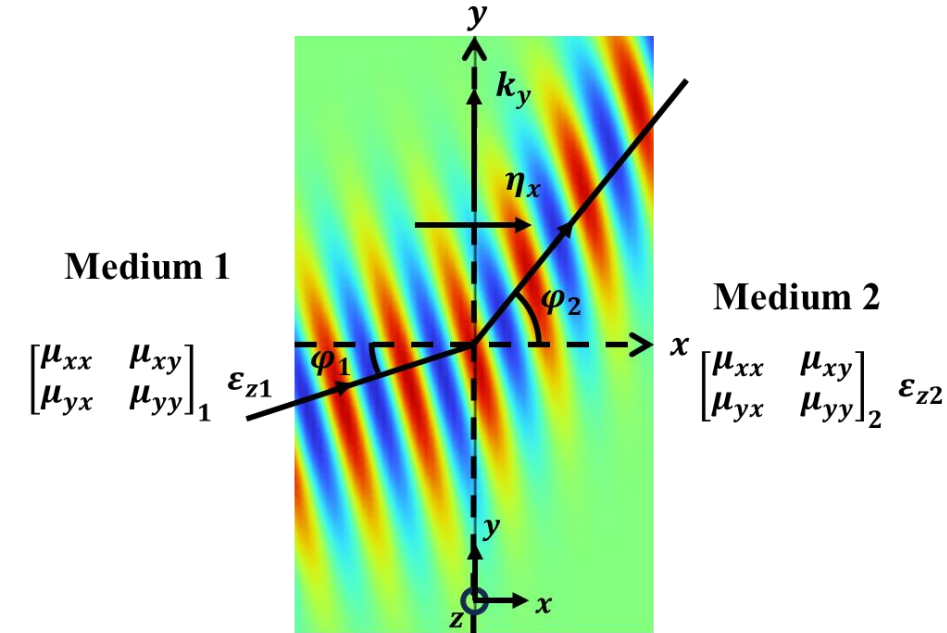
$$\begin{aligned} |\bar{\bar{\mu}}|_1 &= |\bar{\bar{\mu}}|_2 = \Delta, \\ (\mu_{xx}\epsilon_z)_1 &= (\mu_{xx}\epsilon_z)_2 = n_{yy}^2 \end{aligned}$$

$$\bar{\bar{\mu}} = \begin{bmatrix} \mu_{xx} & \mu_{xy} \\ \mu_{xy} & \frac{(\Delta + \mu_{xy}^2)}{\mu_{xx}} \end{bmatrix}, \quad \epsilon_z = \frac{n_{yy}^2}{\mu_{xx}}. \quad (13)$$

The materials can also be rewritten in the following general form,

$$\bar{\bar{\mu}} = \begin{bmatrix} A^{-1} & B \\ B & A(\Delta + B^2) \end{bmatrix}, \quad \epsilon_z = n_{yy}^2 A. \quad (14)$$

Perfect impedance matching reduces the degrees of freedom for a reciprocal, magnetically anisotropic medium from four ($\mu_{xx}, \mu_{xy}, \mu_{yy}, \epsilon_z$) to two (μ_{xx}, μ_{xy}) or equivalently (A, B) , where they share a common Δ and n_{yy}^2 .



$$\bar{\bar{\mu}} = \begin{bmatrix} A^{-1} & B \\ B & A(\Delta + B^2) \end{bmatrix}, \quad \varepsilon_z = n_{yy}^2 A$$

$$\bar{\bar{\mu}} = R^T(\Psi) \sqrt{\Delta} \begin{bmatrix} C & 0 \\ 0 & \frac{1}{C} \end{bmatrix} R(\Psi)$$

Stretching factor C

$$\bar{\bar{\mu}} = \begin{bmatrix} \cos \Psi & -\sin \Psi \\ \sin \Psi & \cos \Psi \end{bmatrix} \sqrt{\Delta} \begin{bmatrix} C & 0 \\ 0 & 1/C \end{bmatrix} \begin{bmatrix} \cos \Psi & \sin \Psi \\ -\sin \Psi & \cos \Psi \end{bmatrix}$$

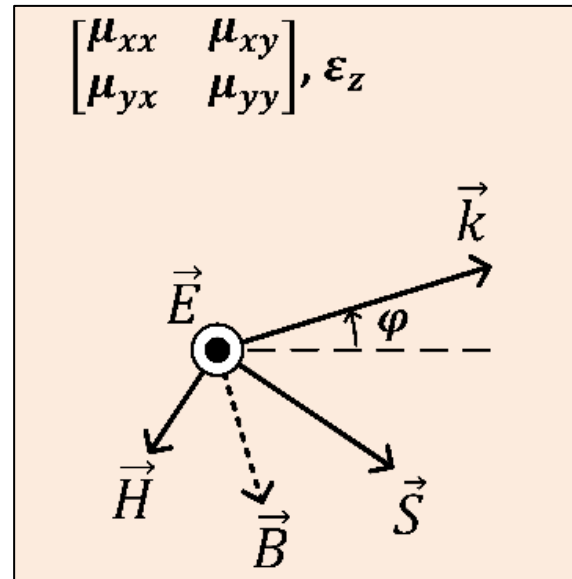
$$\bar{\bar{\mu}} = \sqrt{\Delta} \begin{bmatrix} C \cos^2 \Psi + \frac{1}{C} \sin^2 \Psi & C \sin \Psi \cos \Psi - \frac{1}{C} \sin \Psi \cos \Psi \\ C \sin \Psi \cos \Psi - \frac{1}{C} \sin \Psi \cos \Psi & C \sin^2 \Psi + \frac{1}{C} \cos^2 \Psi \end{bmatrix} \quad (15)$$

$$\varepsilon_z = \frac{n_{yy}^2}{\sqrt{\Delta} (C \cos^2 \Psi + \frac{1}{C} \sin^2 \Psi)} \quad (16)$$

But what can these two degrees of freedom (C, Ψ) or alternatively (A,B) control?

The two degrees of freedom allow us to independently control phase progression and direction of power flow:

$$\vec{k}, \hat{S}$$



Let's have a closer look...

Expressing the material parameters in terms of local phase and power flow

Ampere's Law

$$\varepsilon_z = \begin{bmatrix} \bar{k}_x & \bar{k}_y \end{bmatrix} \begin{bmatrix} 1/\bar{\eta}_x \\ 1/\bar{\eta}_y \end{bmatrix} \quad (5)$$

$$\varepsilon_z = \bar{k}_x \bar{\eta}_x^{-1} + \bar{k}_y \bar{\eta}_y^{-1} \quad (19)$$

$$\bar{\eta}_x = \frac{\bar{k}_x + \kappa \bar{k}_y}{\varepsilon_z} \quad (21) \quad \bar{\eta}_y = \frac{\bar{k}_x + \kappa \bar{k}_y}{\kappa \varepsilon_z} \quad (20)$$

Faraday's Law

$$\begin{bmatrix} \bar{k}_y \\ \bar{k}_x \end{bmatrix} = \begin{bmatrix} \mu_{xx} & -\mu_{xy} \\ -\mu_{yx} & \mu_{yy} \end{bmatrix} \begin{bmatrix} 1/\bar{\eta}_y \\ 1/\bar{\eta}_x \end{bmatrix} \quad (4)$$

$$\mu_{xx} = \bar{k}_y \bar{\eta}_y + \frac{\mu_{xy}}{\kappa} \quad (17)$$

$$\mu_{yy} = \bar{k}_x \bar{\eta}_x + \mu_{xy} \kappa \quad (18)$$

where $\kappa = \bar{\eta}_x / \bar{\eta}_y = \tan \theta_S$

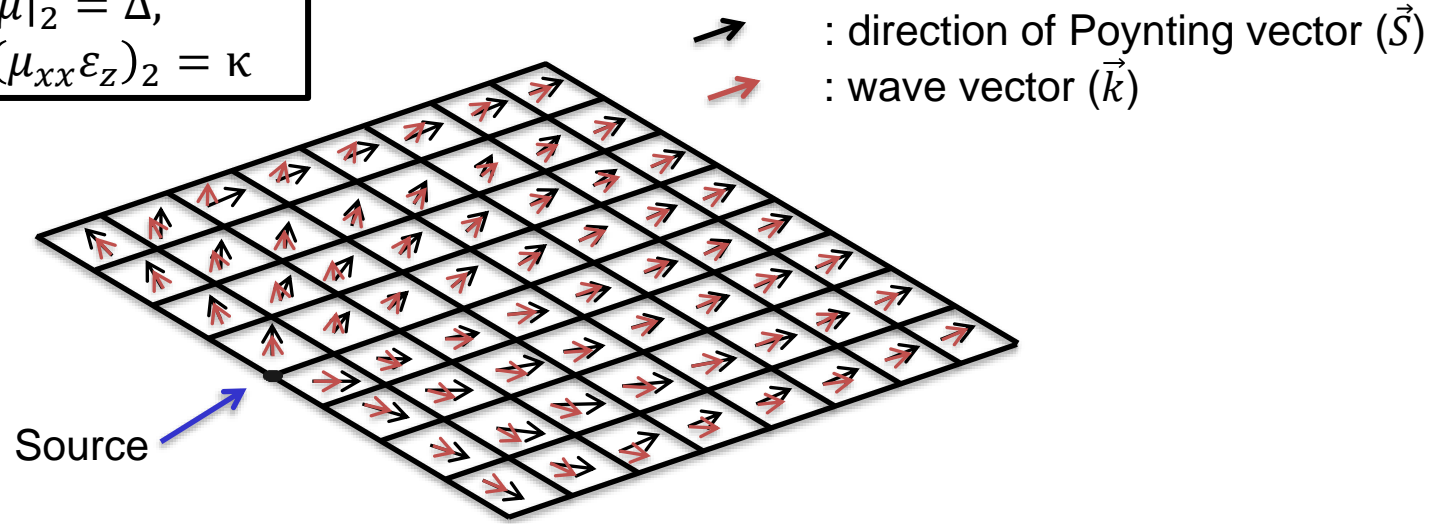
defines the direction of the power flow with respect to the x -axis

$$\bar{\bar{\mu}} = \begin{bmatrix} \frac{\bar{k}_y}{\varepsilon_z} \left(\frac{\bar{k}_x}{\kappa} + \bar{k}_y \right) + \frac{\mu_{xy}}{\kappa} & \mu_{xy} \\ \mu_{xy} & \frac{\bar{k}_x}{\varepsilon_z} (\bar{k}_x + \kappa \bar{k}_y) + \kappa \mu_{xy} \end{bmatrix} \quad (22)$$

Material parameters solely in terms of local phase progression and power flow direction

Applying,

$$\begin{aligned} |\bar{\mu}|_1 &= |\bar{\mu}|_2 = \Delta, \\ (\mu_{xx}\varepsilon_z)_1 &= (\mu_{xx}\varepsilon_z)_2 = \kappa \end{aligned}$$



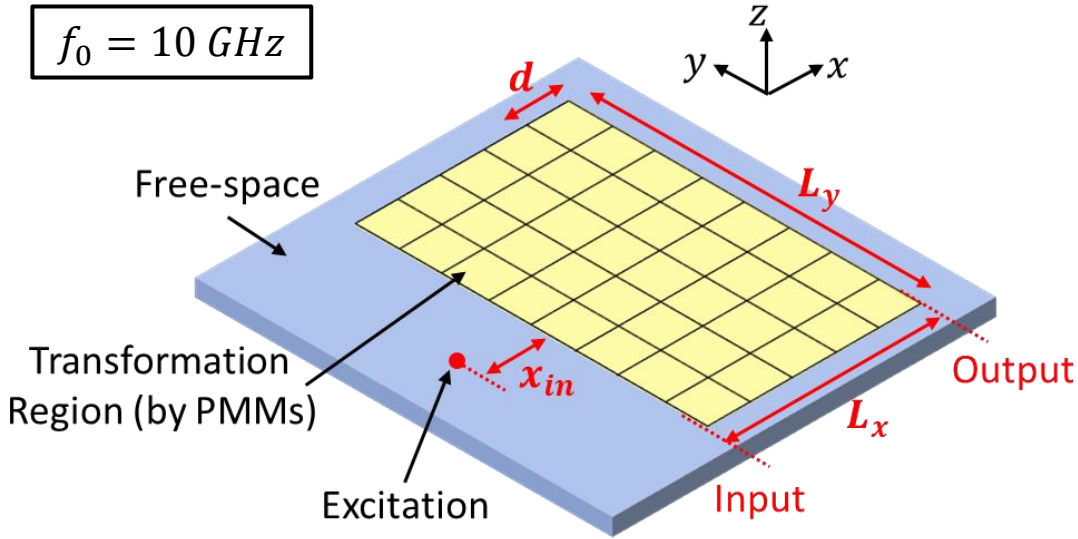
$$\bar{\mu} = \begin{bmatrix} \frac{\varepsilon_z \Delta}{(\bar{k}_x + \kappa \bar{k}_y)^2} + \frac{\bar{k}_y^2}{\varepsilon_z} & \frac{\kappa \varepsilon_z \Delta}{(\bar{k}_x + \kappa \bar{k}_y)^2} - \frac{\bar{k}_x \bar{k}_y}{\varepsilon_z} \\ \frac{\kappa \varepsilon_z \Delta}{(\bar{k}_x + \kappa \bar{k}_y)^2} - \frac{\bar{k}_x \bar{k}_y}{\varepsilon_z} & \frac{\kappa^2 \varepsilon_z \Delta}{(\bar{k}_x + \kappa \bar{k}_y)^2} + \frac{\bar{k}_x^2}{\varepsilon_z} \end{bmatrix} \quad (23)$$

$$\varepsilon_z = (\bar{k}_x + \kappa \bar{k}_y) \sqrt{\frac{n_{yy}^2 - k_y^2}{\Delta}} \quad (24)$$

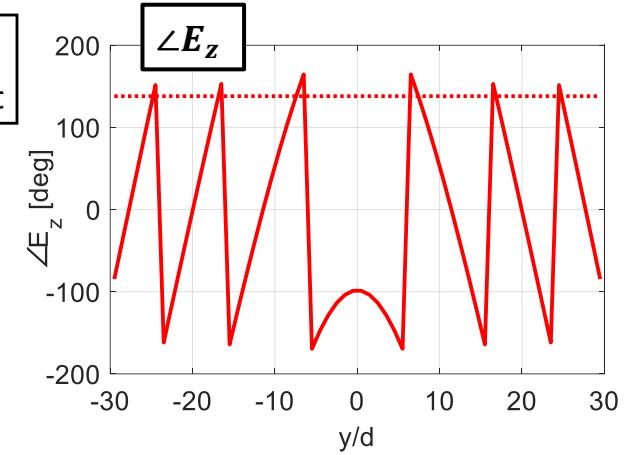
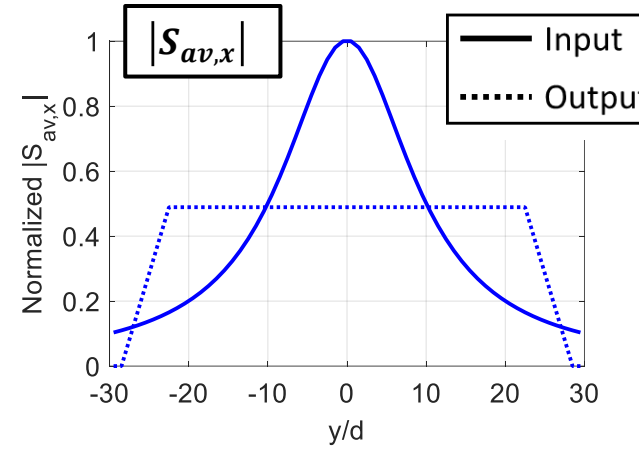
The material parameters can be defined solely in terms of local phase progression and power flow direction.

Example: Perfectly-matched Collimator

$$f_0 = 10 \text{ GHz}$$



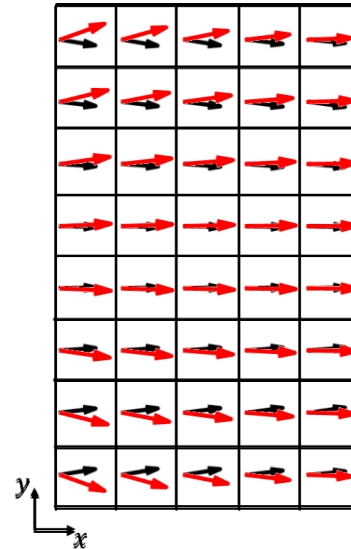
$$d = \lambda_0/7.2; L_x = 1.4\lambda_0, L_y = 8.4\lambda_0; x_{in} = 10d = 1.4\lambda_0$$



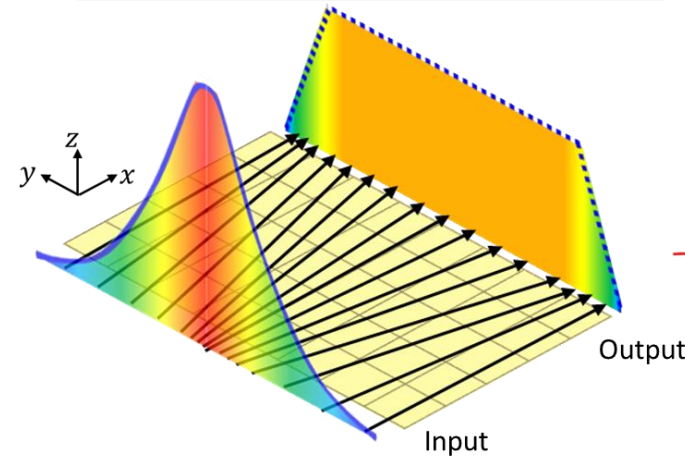
Stipulate output and input field.

Obtain local power direction (κ) and phase progression (\bar{k}_x, \bar{k}_y).

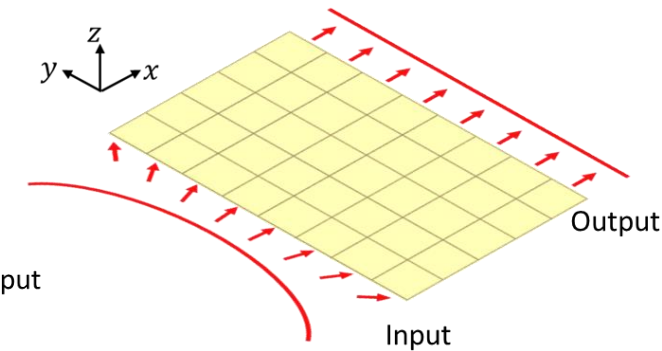
Calculate $\bar{\mu}, \epsilon_z$



Direction of Power Flow (\hat{S})



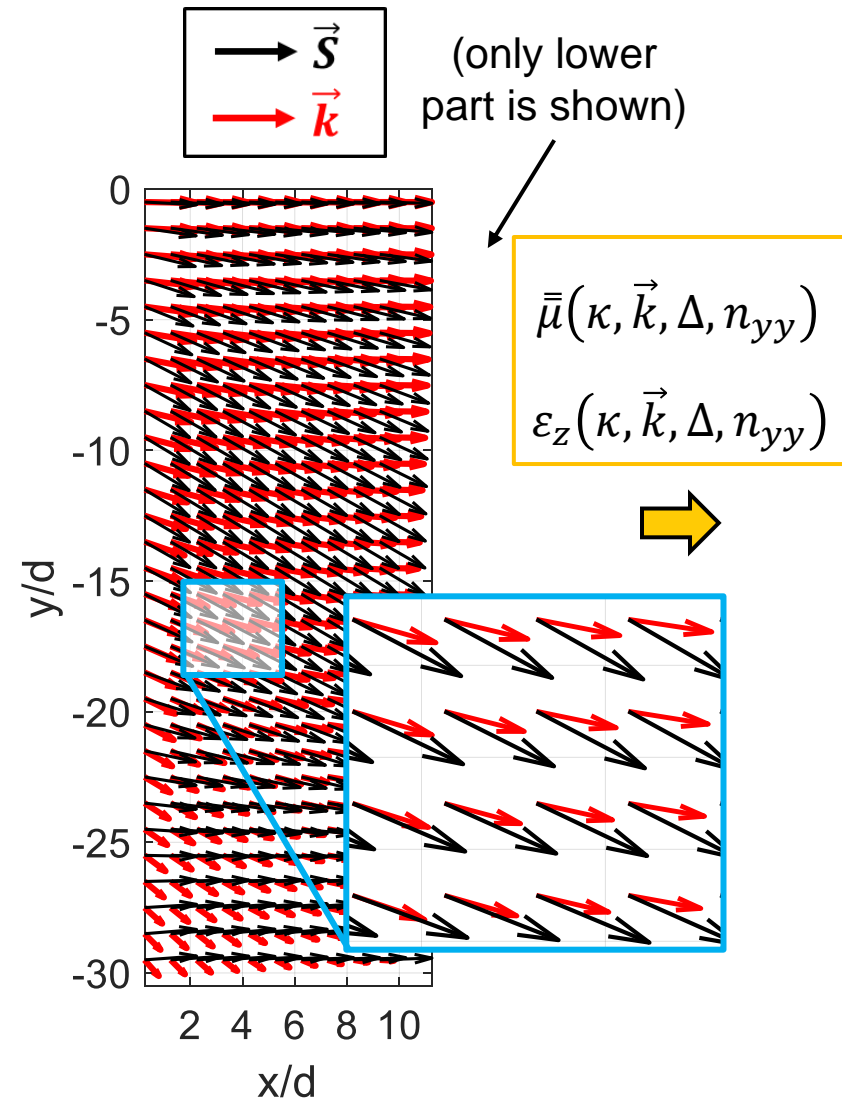
Phase progression (\bar{k})



Perfectly-matched Collimator

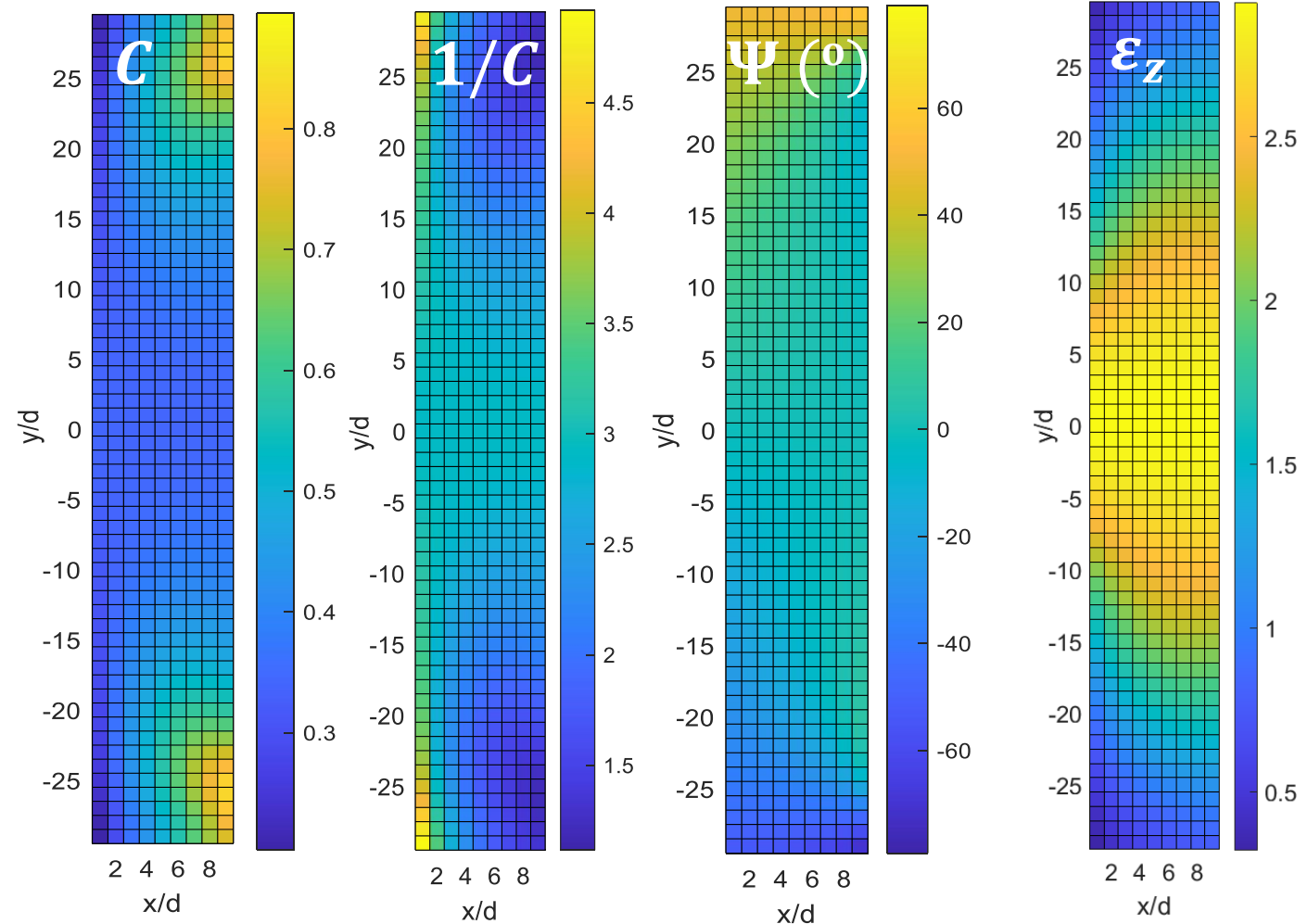


$$f_0 = 10 \text{ GHz}; d = \lambda_0/7.2; L_x = 1.4\lambda_0, L_y = 8.4\lambda_0; x_{in} = 10d; \Delta = n_{yy}^2 = 1.$$



$$\bar{\mu}(x, y) = R^T(\Psi) \begin{bmatrix} C & 0 \\ 0 & \frac{1}{C} \end{bmatrix} R(\Psi)$$

$$\varepsilon_z(x, y)$$

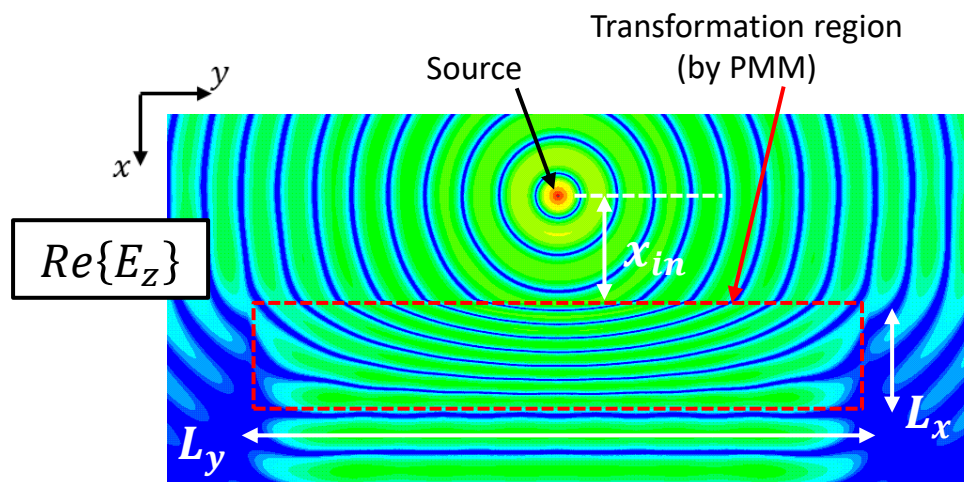
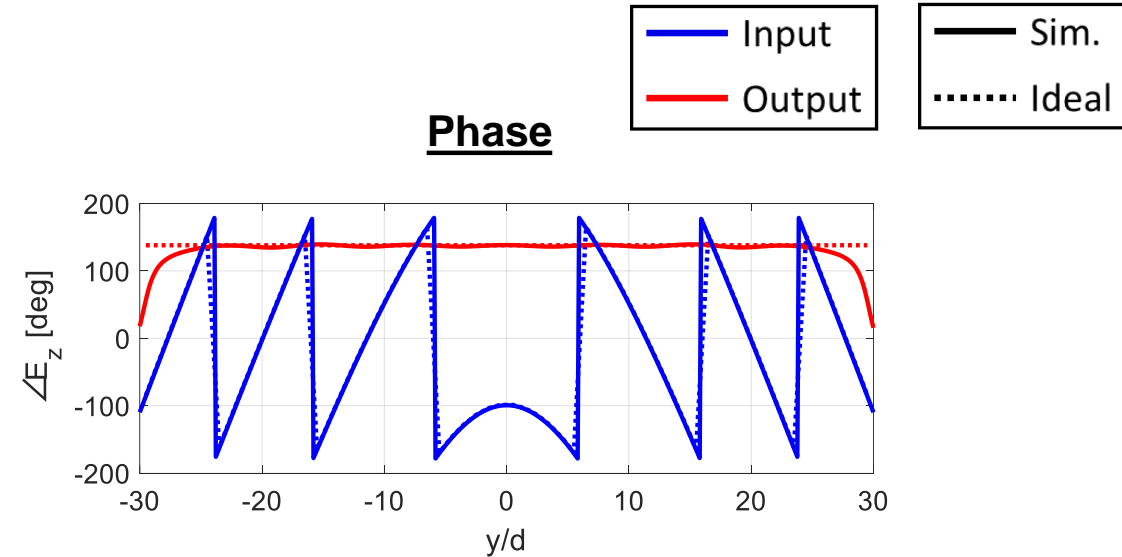
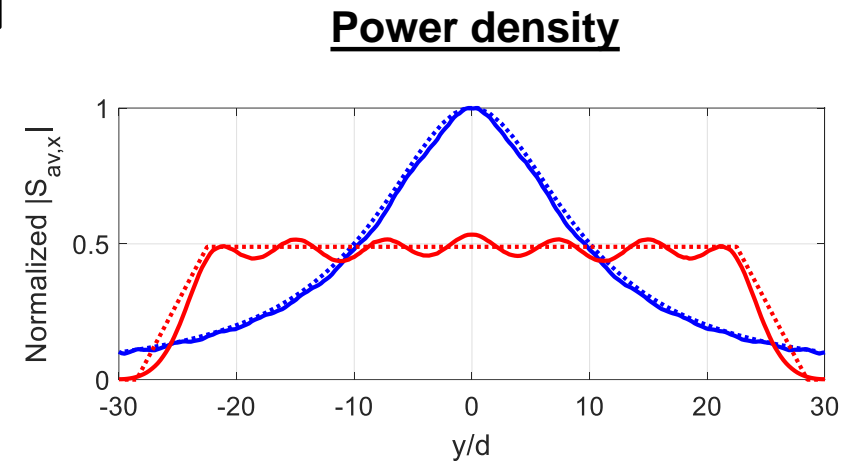
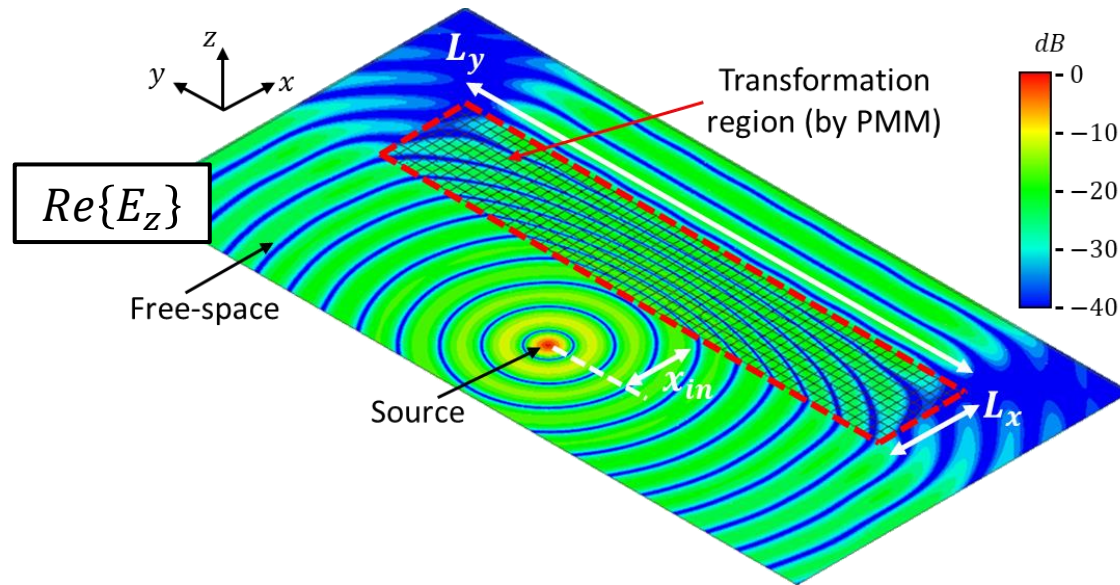


Collimator Simulations

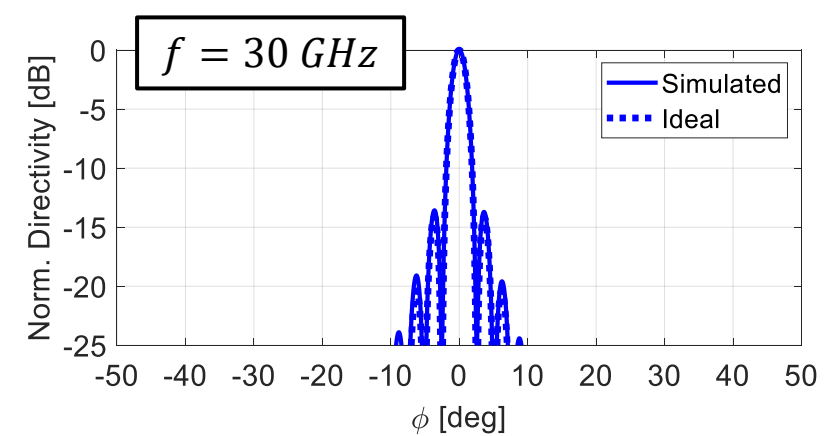
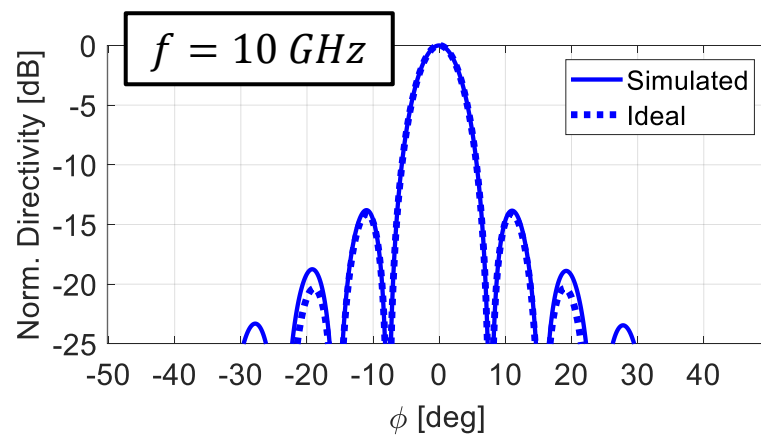
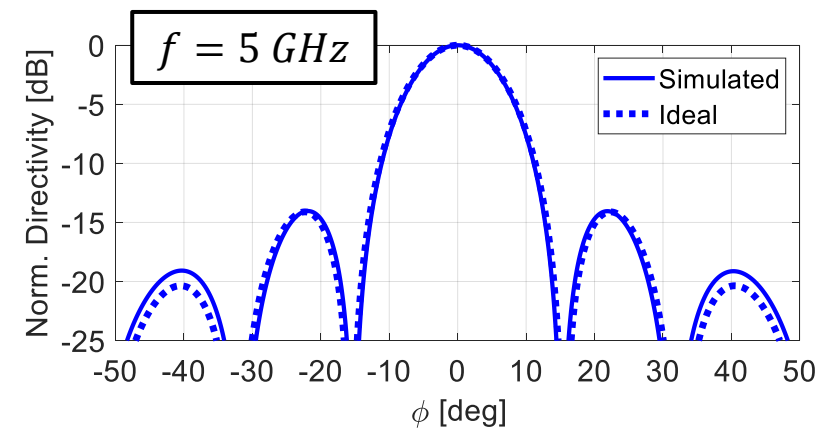
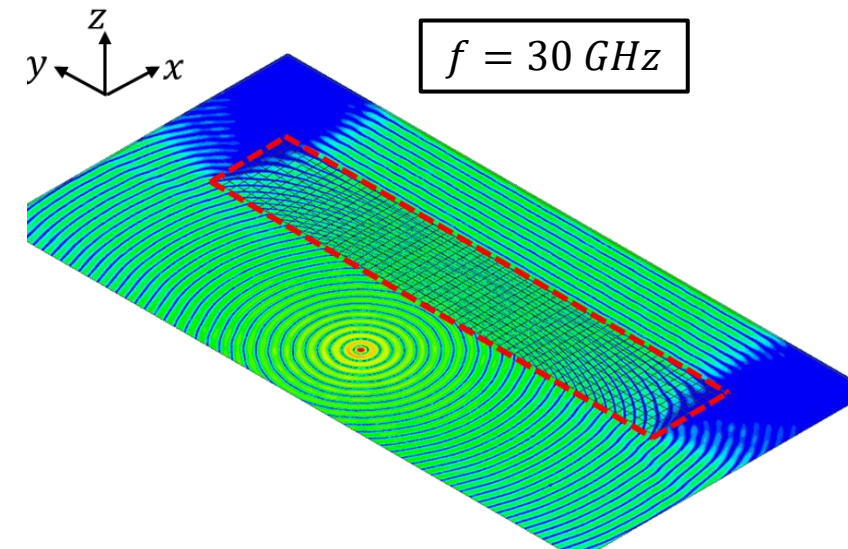
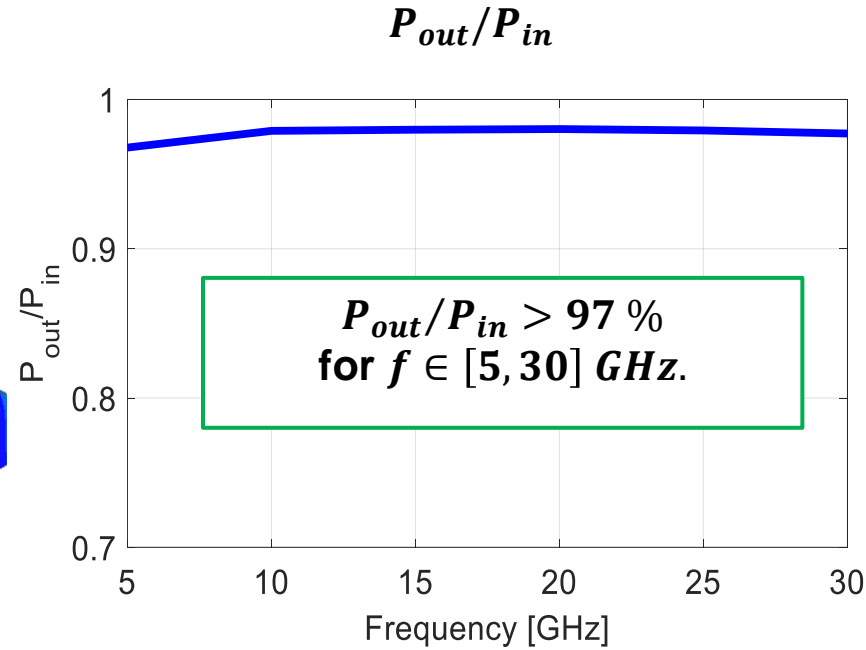
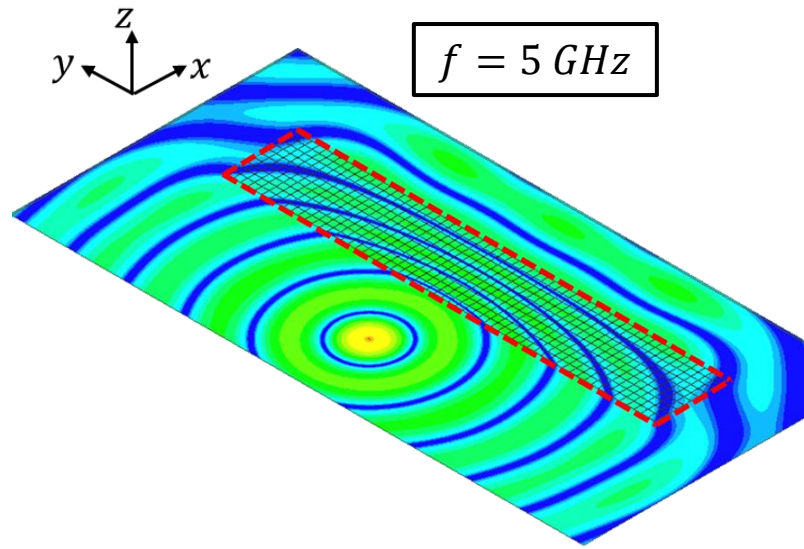


$$d = \lambda_0/7.2; L_x = 1.4\lambda_0, L_y = 8.4\lambda_0; x_{in} = 10d; \Delta = n_{yy}^2 = 1.$$

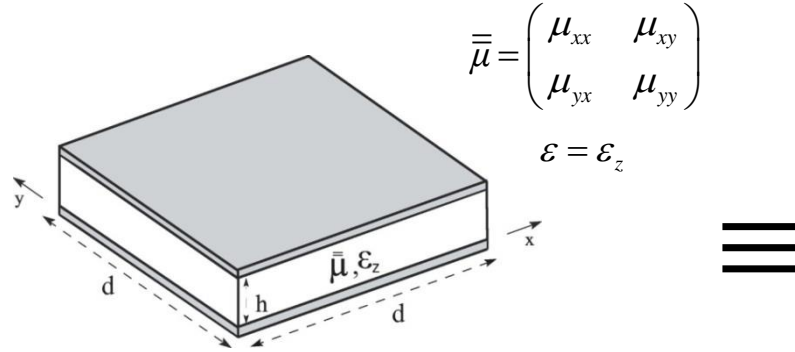
$$f_0 = 10 \text{ GHz}$$



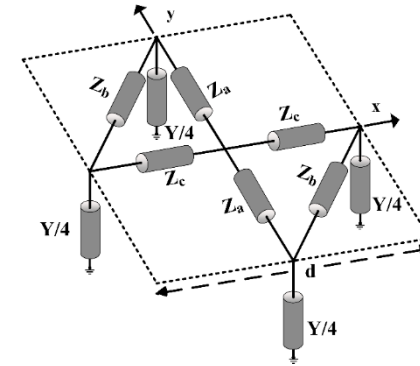
Collimator Bandwidth



Parallel Plate Waveguide



Tensor Transmission-Line (TL) Unit Cell



Permeability Tensor

$$j\omega d \begin{pmatrix} \mu_{yy} & -\mu_{xy} \\ -\mu_{yx} & \mu_{xx} \end{pmatrix} \Leftrightarrow$$

Impedance Tensor

$$\bar{Z} = \begin{pmatrix} Z_{xx} & Z_{xy} \\ Z_{yx} & Z_{yy} \end{pmatrix} = \begin{pmatrix} \frac{1}{2Z_b} + \frac{1}{2Z_c} & \frac{1}{2Z_b} \\ \frac{1}{2Z_b} & \frac{1}{2Z_a} + \frac{1}{2Z_b} \end{pmatrix}^{-1}$$

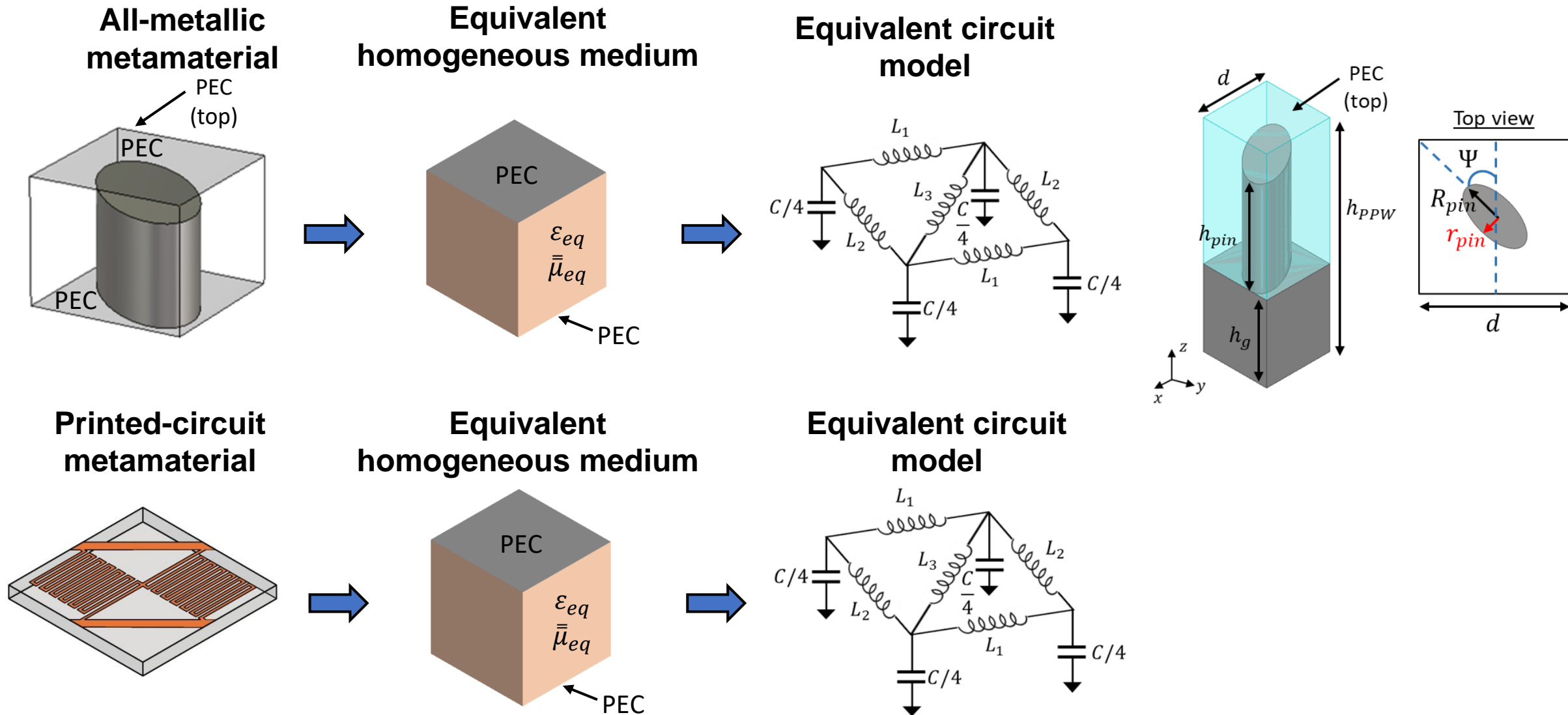
Permittivity Scalar

$$j\omega d \epsilon_z \Leftrightarrow$$

Admittance Scalar

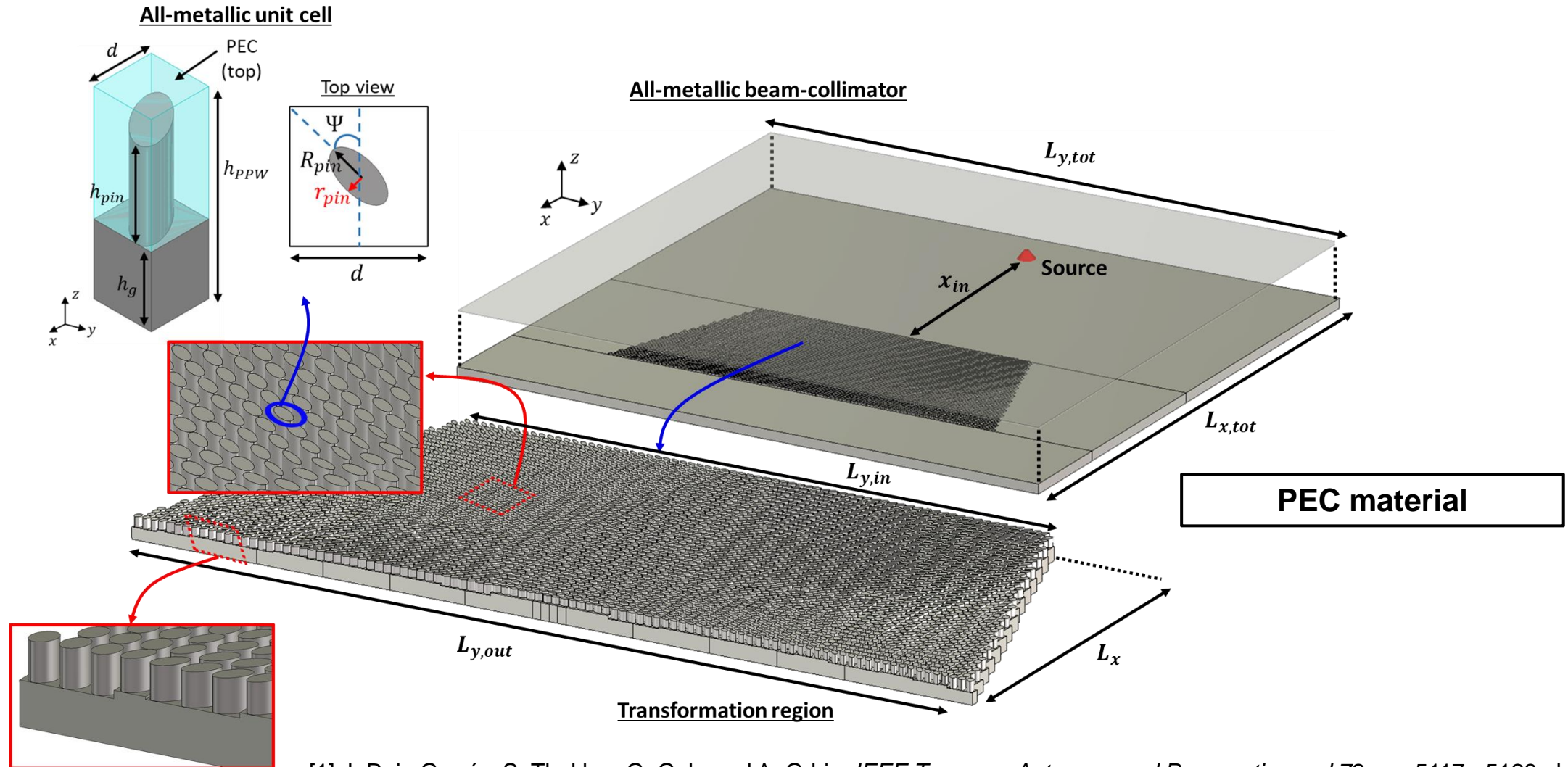
$$Y$$

- [1] G. Gok and A. Grbic, "Tensor transmission-line metamaterials", *IEEE Trans. on Antennas and Propagation*, vol. 58, no. 5, pp. 1559-1566, May 2010.
- [2] M. Zedler and G. V. Eleftheriades, "Anisotropic transmission-line metamaterials for 2-D transformation optics applications," *Proceedings of the IEEE*, 99, 10, pp. 1634-1645, Oct. 2011.
- [3] D. H. Kwon and C.D. Emiroglu, "Non-orthogonal grids in two-dimensional transmission-line metamaterials," *IEEE Trans. on Antennas and Propagation*, vol. 60, no. 9, pp. 4210-4218, 2012.

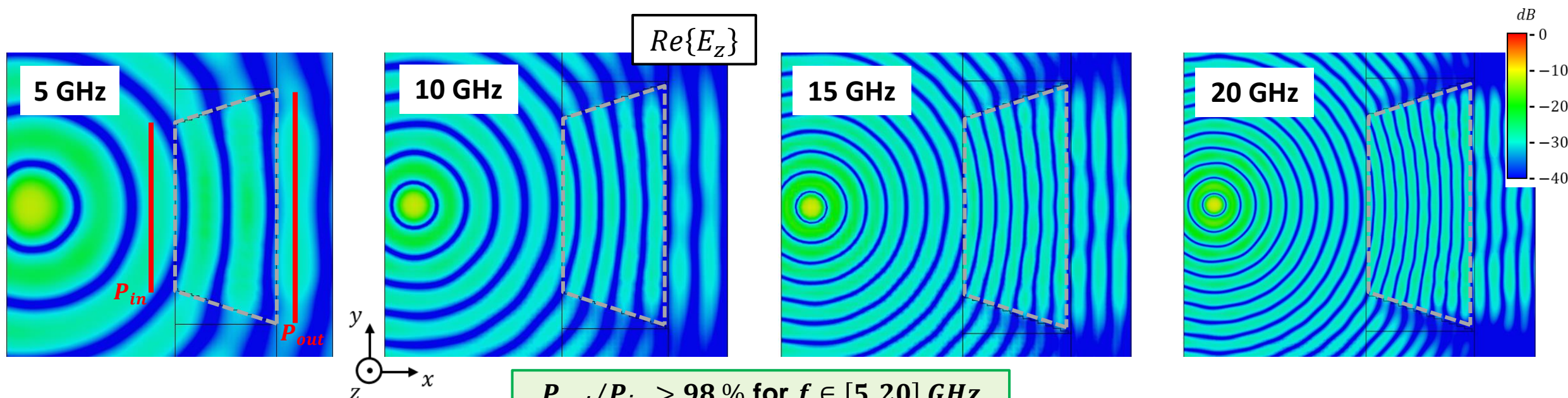


[1] J. Ruiz-García, S. Thakkar, G. Gok, and A. Grbic. "All-Metal Tensor Metamaterials: Characterization and Design." *IEEE Trans. on Antennas and Propagation*, vol 72, pp. 5117 - 5128, Jun. 2024.

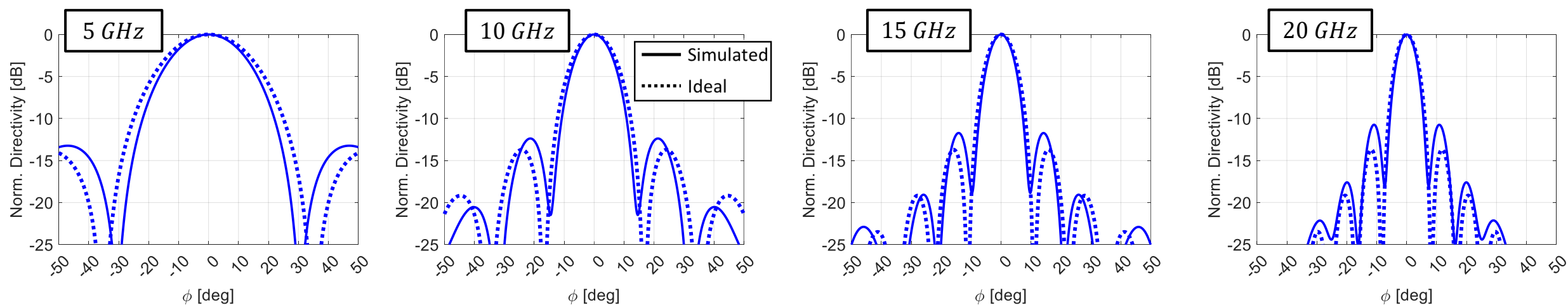
[2] G. Gok and A. Grbic, *IEEE Trans. on Antennas and Propagation*, vol. 61, pp. 728-734, February 2013.



Simulated Performance Over Bandwidth



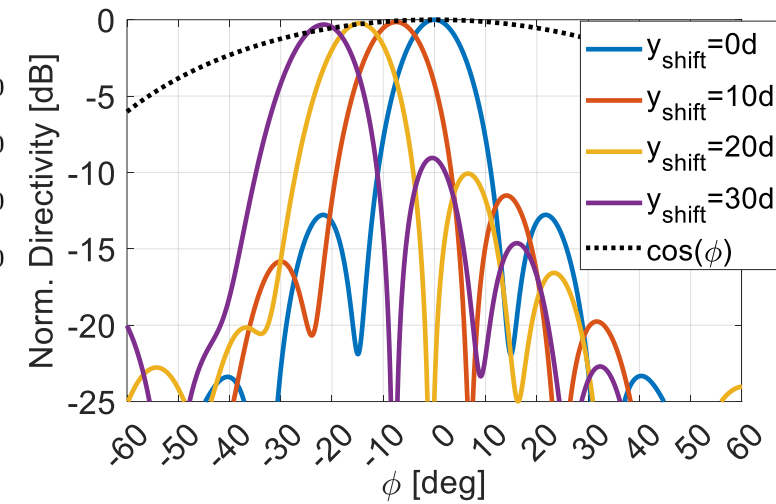
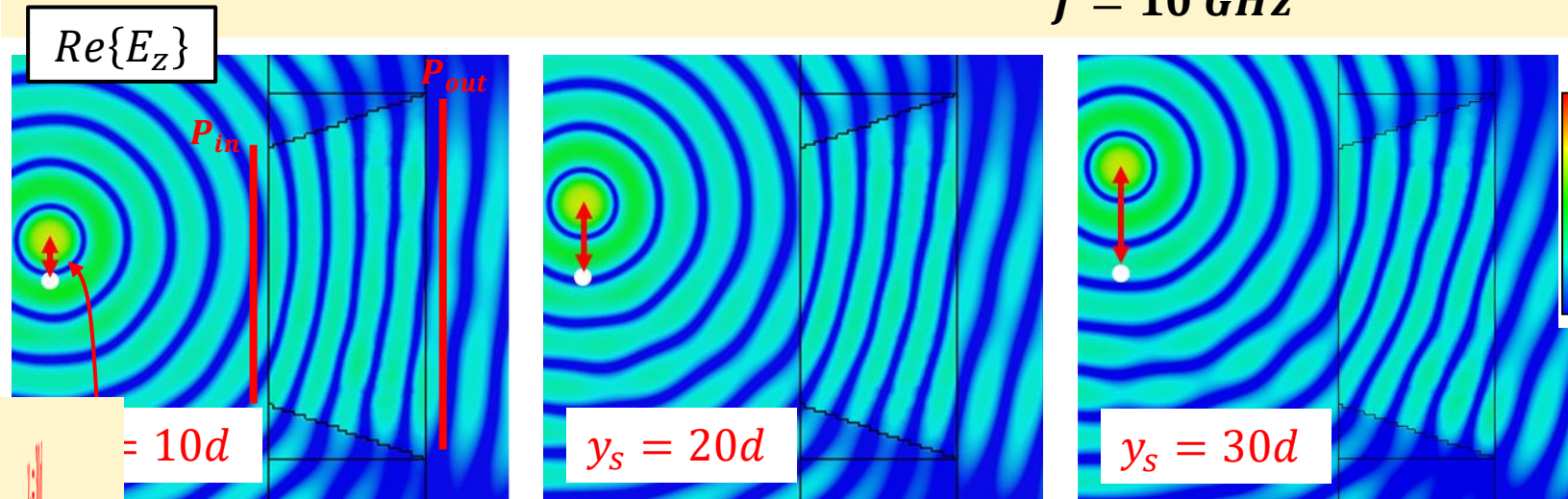
$P_{out}/P_{in} > 98\%$ for $f \in [5, 20]$ GHz
(assuming no losses).



Simulated Scanning Performance

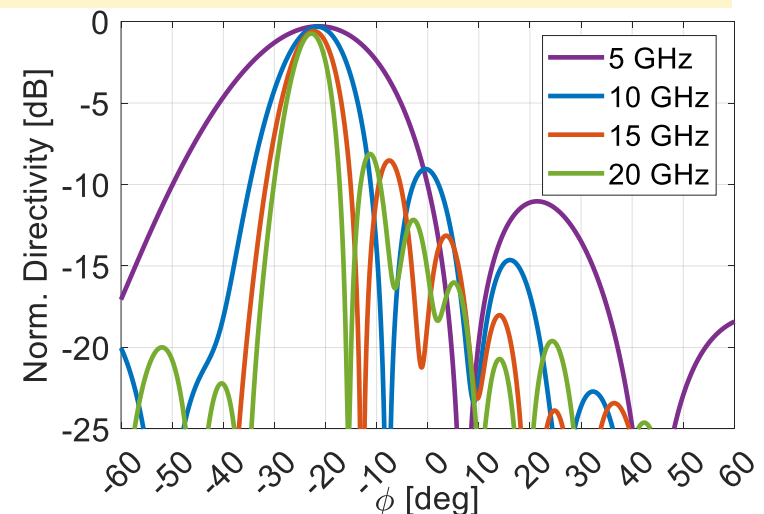
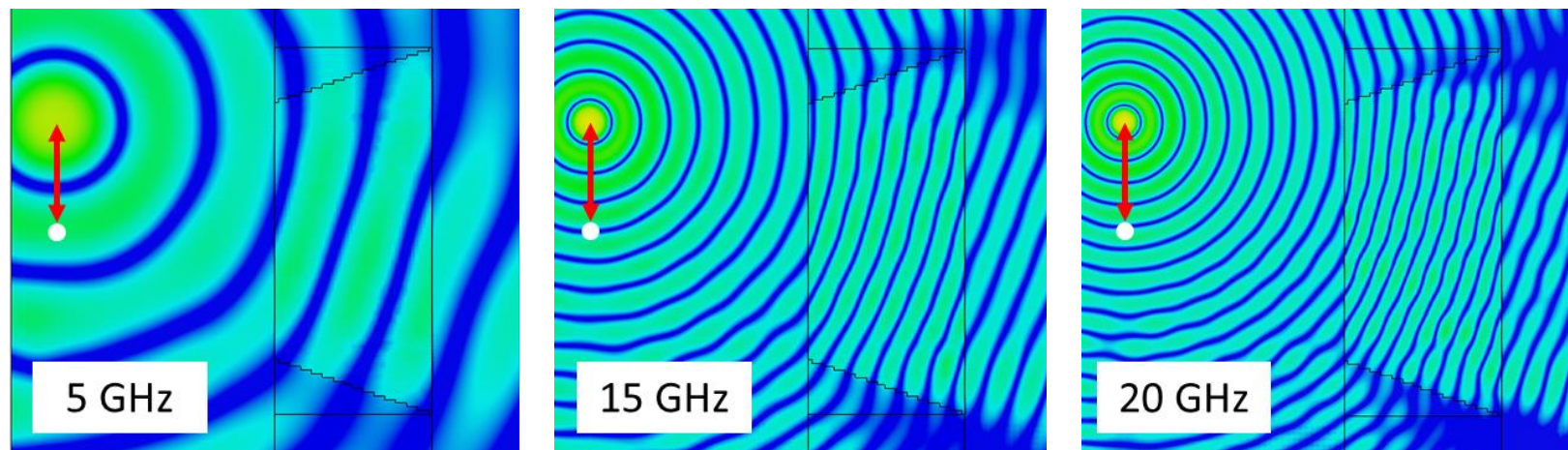
$f = 10 \text{ GHz}$

$\Delta D = -0.3 \text{ dB}, \phi_0 \in [-22^\circ, 22^\circ]$



$P_{out}/P_{in} > 95 \%$ for $f \in [5, 20] \text{ GHz}$ and $y_s \in [0, 30d]$ (assuming no losses).

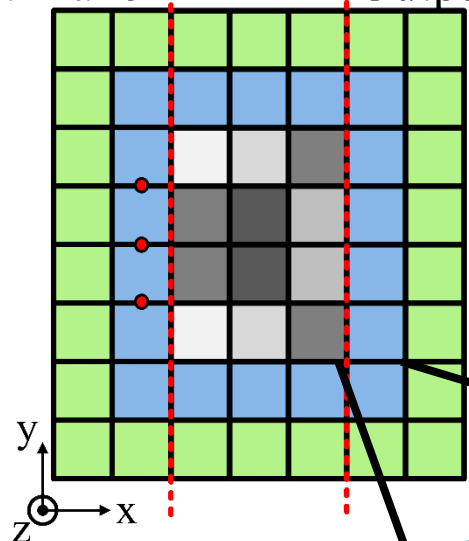
$y_s = 30d$



Inverse design of perfectly-matched metamaterials through circuit synthesis

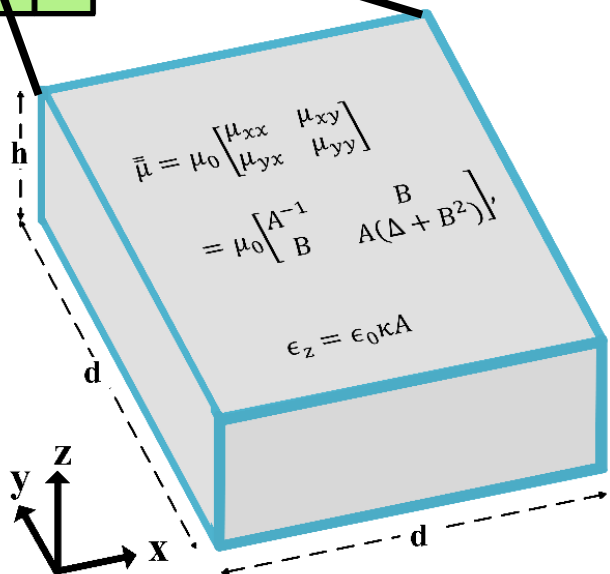


Input Plane Output Plane

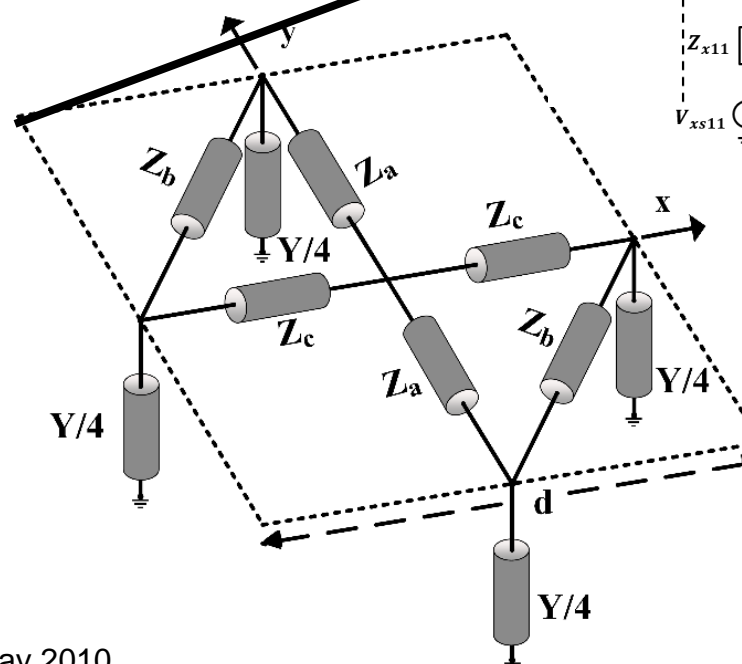
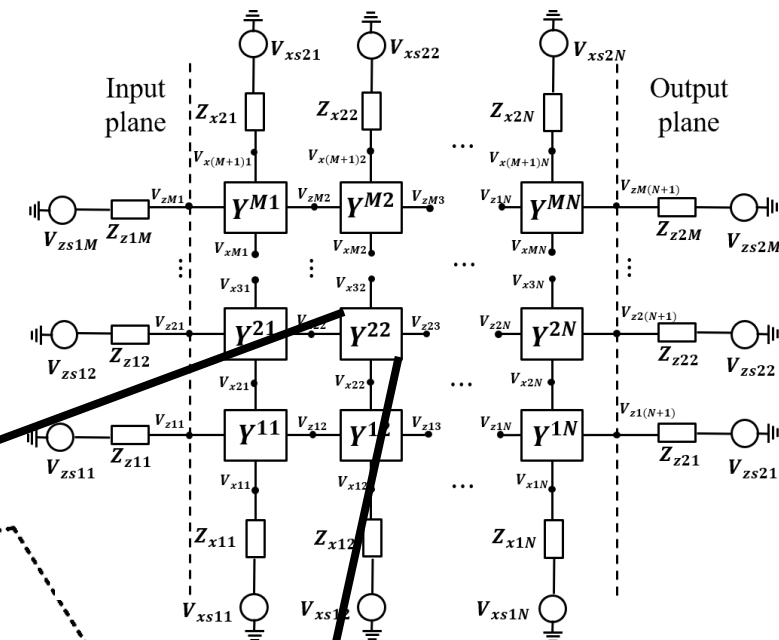


2-D Perfectly Matched Metamaterial

Perfectly-Matched Media



2-D Circuit Network [2]

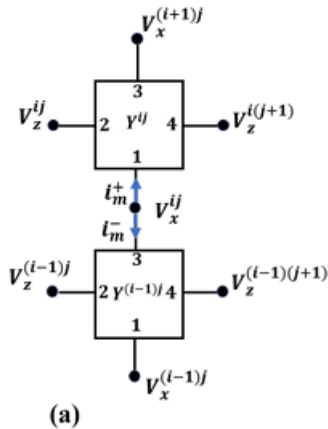
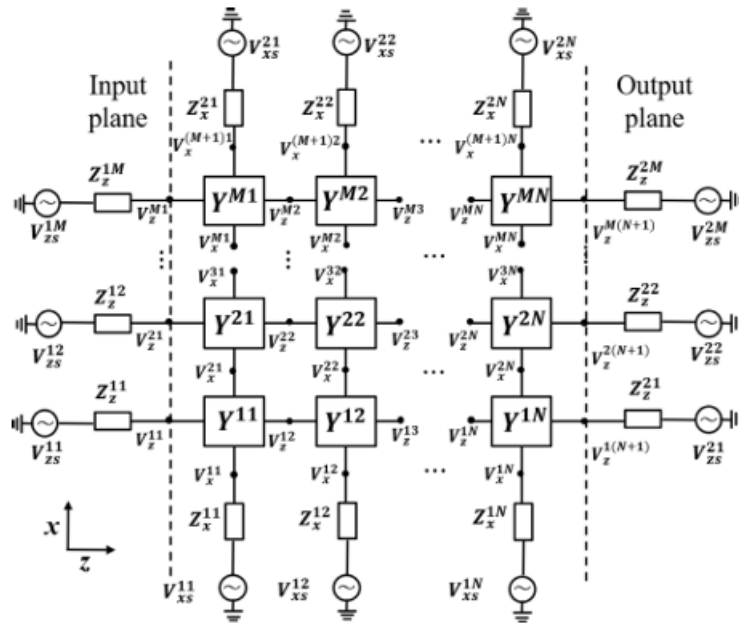


Tensor Transmission-Line Unit Cell [1]

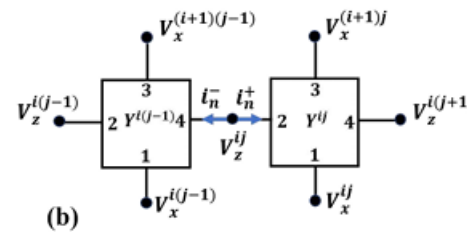
[1] G. Gok and A. Grbic, *IEEE Trans. Antennas Propag.*, vol. 58, no. 5, pp. 1559–1566, May 2010

[2] L. Szymanski, G. Gok and A. Grbic, *IEEE Trans. Antennas Propag.*, Dec. 2021.

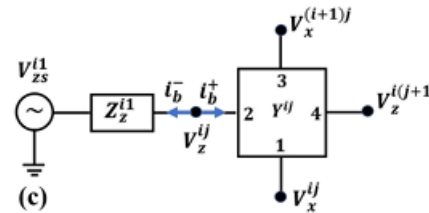
The Interaction Matrix $\bar{\bar{Q}}$



$$V_x^{ij} \left(Y_{11}^{ij} + Y_{33}^{(i-1)j} \right) + V_x^{(i-1)j} Y_{31}^{(i-1)j} + V_x^{(i+1)j} Y_{13}^{ij} + V_z^{ij} Y_{12}^{ij} + V_z^{(i-1)j} Y_{32}^{(i-1)j} + V_z^{(i-1)(j+1)} Y_{34}^{(i-1)j} + V_z^{(i+1)(j+1)} Y_{14}^{ij} = 0.$$



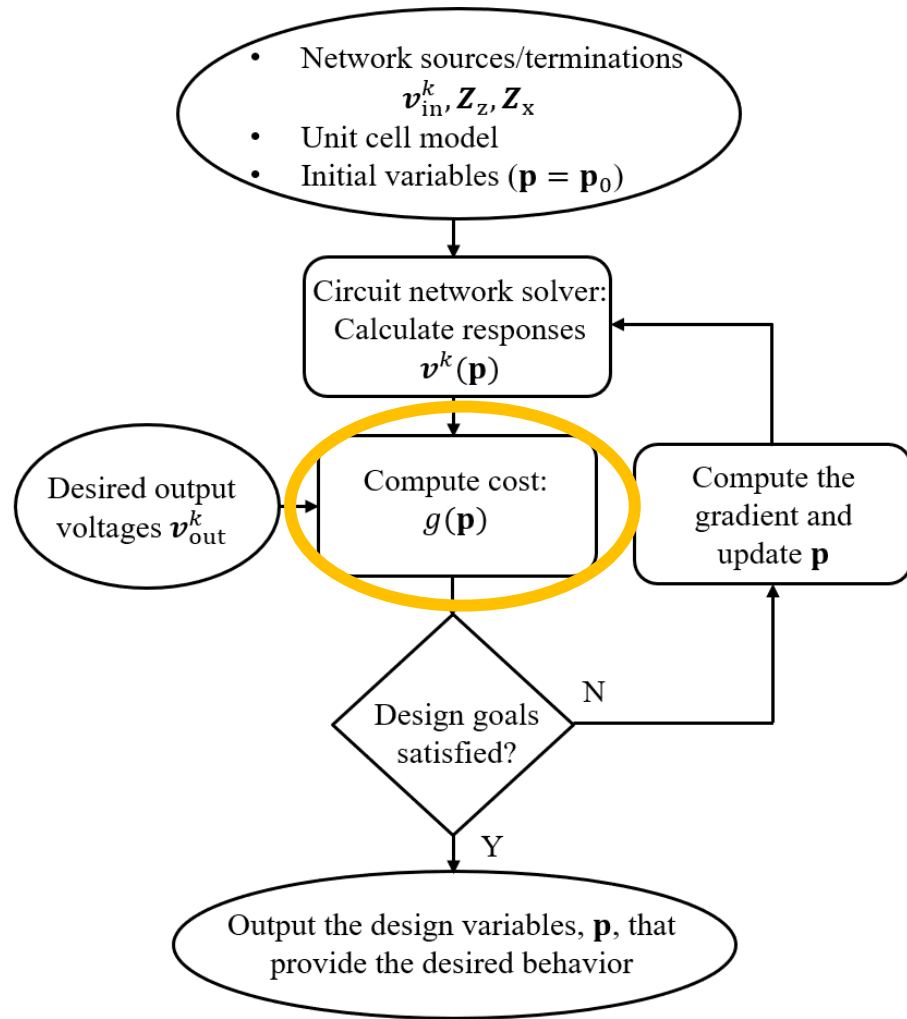
$$V_z^{ij} \left(Y_{22}^{ij} + Y_{44}^{i(j-1)} \right) + V_z^{i(j-1)} Y_{42}^{i(j-1)} + V_z^{i(j+1)} Y_{24}^{ij} + V_x^{ij} Y_{21}^{ij} + V_x^{(i+1)j} Y_{23}^{ij} + V_x^{(i+1)(j-1)} Y_{43}^{i(j-1)} + V_x^{i(j-1)} Y_{41}^{i(j-1)} = 0.$$



$$V_z^{i1} \left(Y_{22}^{i1} + \frac{1}{Z_z^{i1}} \right) + V_z^{i2} Y_{24}^{i1} + V_x^{i1} Y_{21}^{i1} + V_x^{(i+1)1} Y_{23}^{i1} = \frac{V_{zs}^{i1}}{Z_z^{i1}}$$

- Forward Problem: $\bar{\bar{Q}}^k \mathbf{v}^k(\mathbf{p}) = \mathbf{v}_{in}^k$
- $\bar{\bar{Q}}$ characterizes the interactions between the unit cells in the network
- It is a sparse matrix composed of admittance matrix entries as shown here

Inverse design procedure – cost function



- For a K -Input K -Output device, we stipulate the following:

$$v_{in}^k, v_{out}^k, \text{ where } k \in \{1, 2, 3, \dots, K\}$$

- Forward Problem: $\bar{Q}^k \mathbf{v}^k(\mathbf{p}) = \mathbf{v}_{in}^k$

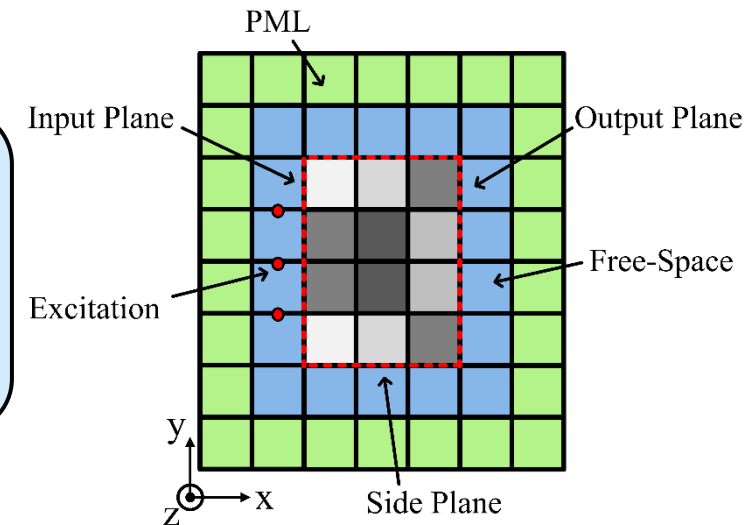
- Cost function definition:

$$g(\mathbf{p}) = \sum_{k=1}^K \frac{1}{2} (\mathbf{v}^k(\mathbf{p}) - \mathbf{v}_{out}^k)^H \bar{G} (\mathbf{v}^k(\mathbf{p}) - \mathbf{v}_{out}^k)$$

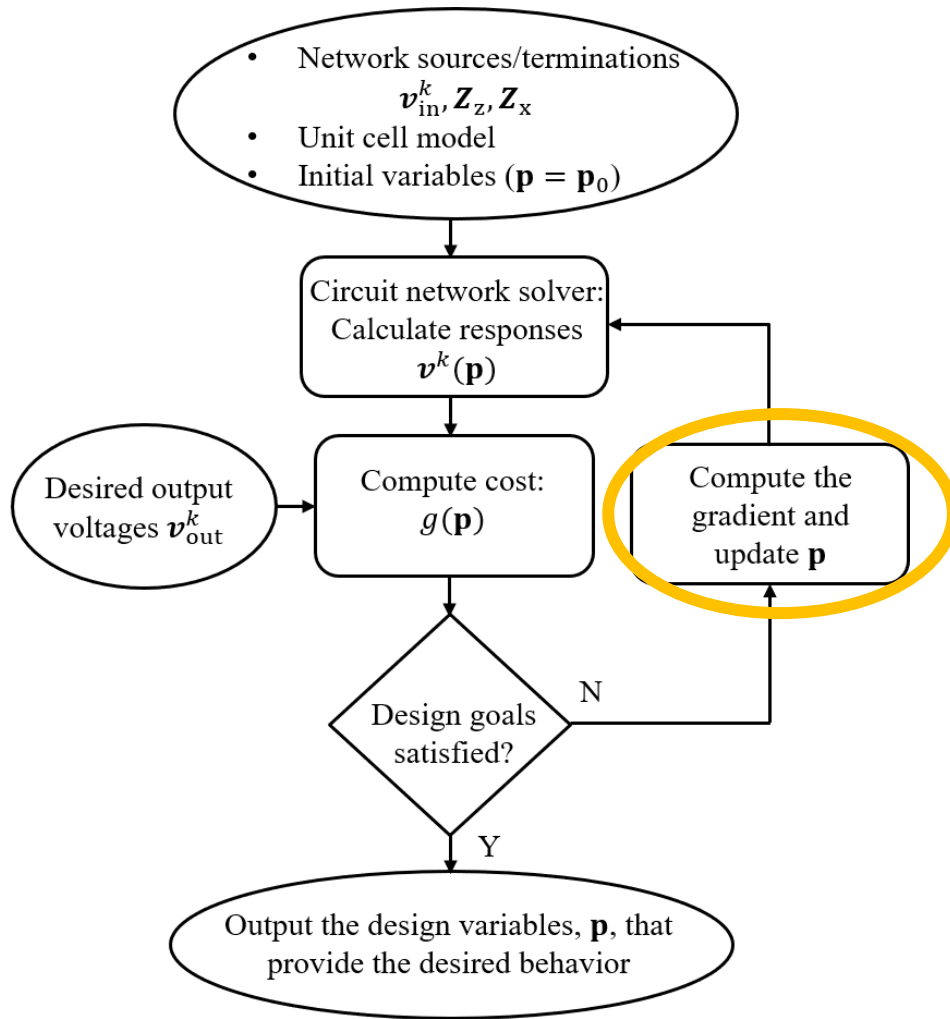
\mathbf{p} : Vector of P variables

$\mathbf{v}^k(\mathbf{p})$: Response to k^{th} input

\bar{G} : Positive semi-definite matrix



Inverse design procedure – adjoint method



\mathbf{p} : Vector of P variables
 $\mathbf{v}^k(\mathbf{p})$: Response to k^{th} input
 $\bar{\bar{G}}$: Positive semi-definite matrix

- Cost function definition:

$$g(\mathbf{p}) = \sum_{k=1}^K \frac{1}{2} (\mathbf{v}^k(\mathbf{p}) - \mathbf{v}_{out}^k)^H \bar{\bar{G}} (\mathbf{v}^k(\mathbf{p}) - \mathbf{v}_{out}^k)$$

- Forward Problem:

$$\bar{\bar{Q}}^k \mathbf{v}^k(\mathbf{p}) = \mathbf{v}_{in}^k$$

- The Gradient:

$$\nabla_{\mathbf{p}}(g) = - \sum_{k=1}^K \text{Re}\{\lambda_k^H \bar{\bar{V}}_{\mathbf{p}}^k\}$$

Adjoint Problem [1]:

$$(\bar{\bar{Q}}^k)^H \lambda_k = \bar{\bar{G}} (\mathbf{v}^k(\mathbf{p}) - \mathbf{v}_{out}^k)$$

Therefore, the Gradient costs $2 \times K$ forward solutions

$$\bar{\bar{V}}_{\mathbf{p}}^k = \nabla_{\mathbf{p}} \bar{\bar{Q}}^k \mathbf{v}^k(\mathbf{p})$$

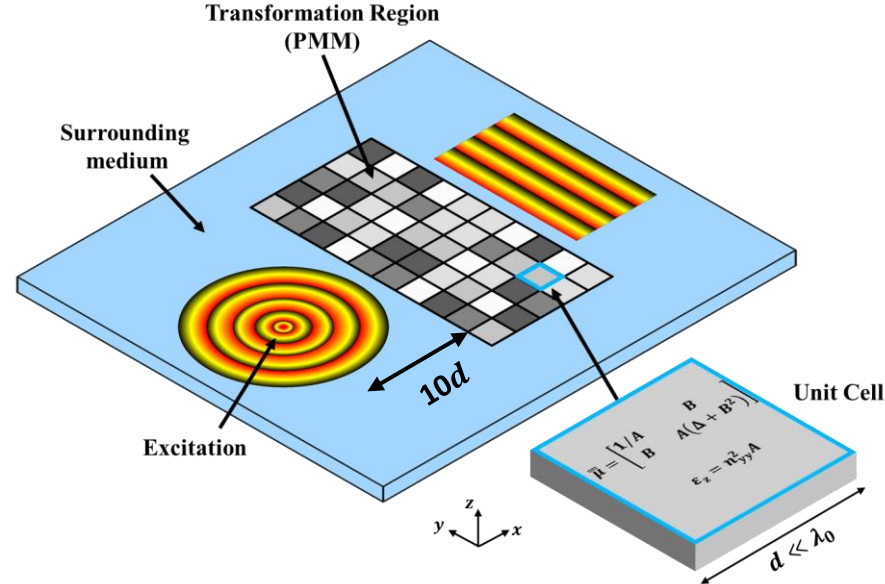
$$\bar{\bar{V}}_{\mathbf{p}}^k = \left[\frac{\partial \bar{\bar{Q}}^k}{\partial p_1} \mathbf{v}^k \mid \frac{\partial \bar{\bar{Q}}^k}{\partial p_2} \mathbf{v}^k \mid \dots \frac{\partial \bar{\bar{Q}}^k}{\partial p_P} \mathbf{v}^k \right]$$

[1] C. M. Lalau-Keraly, S. Bhargava, O. D. Miller, and E. Yablonovitch, *Opt. Express*, Sep. 2013.

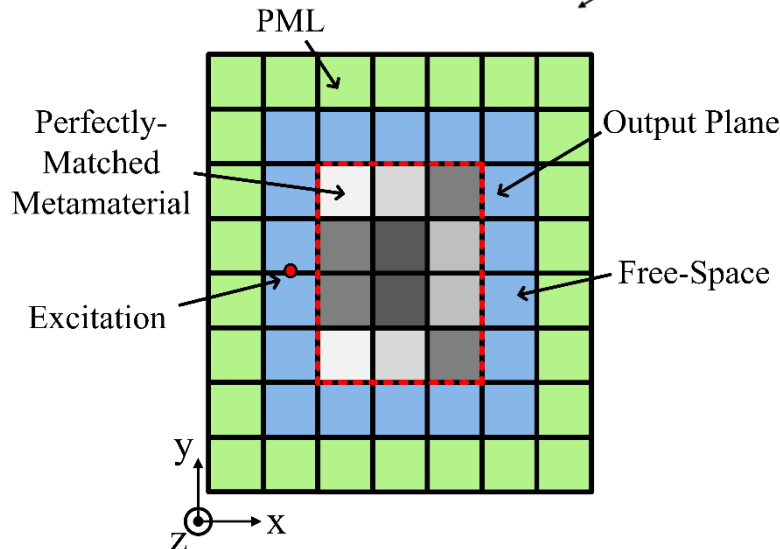
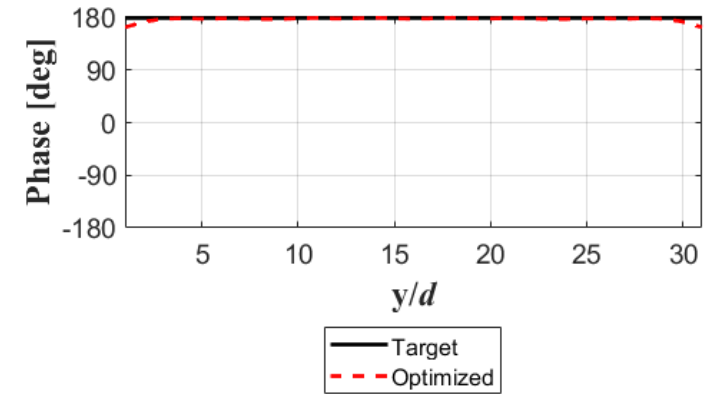
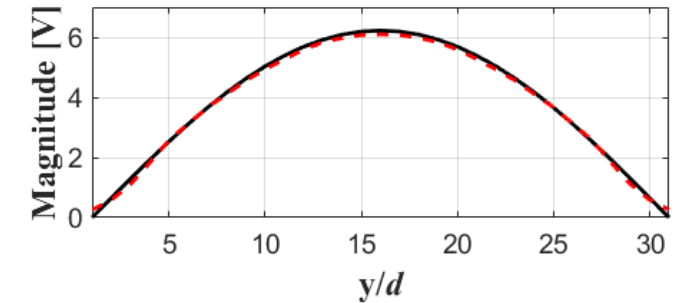
[2] S. Thakkar, J. Ruiz-García, L. Szymanski, G. Gok, and A. Grbic, "Beamforming with Perfectly-Matched Metamaterials," *European Conference on Antennas and Propagation (EuCAP)*, accepted, Stockholm, Sweden, submitted Sept 2024.

Inverse design: beam collimator with amplitude control

- Cosine amplitude taper.
- The computational domain consists of the PMM (greyscale), free space (blue) and PML terminations (green).
- Symmetry is imposed across the centerline due to the symmetry of the aperture field



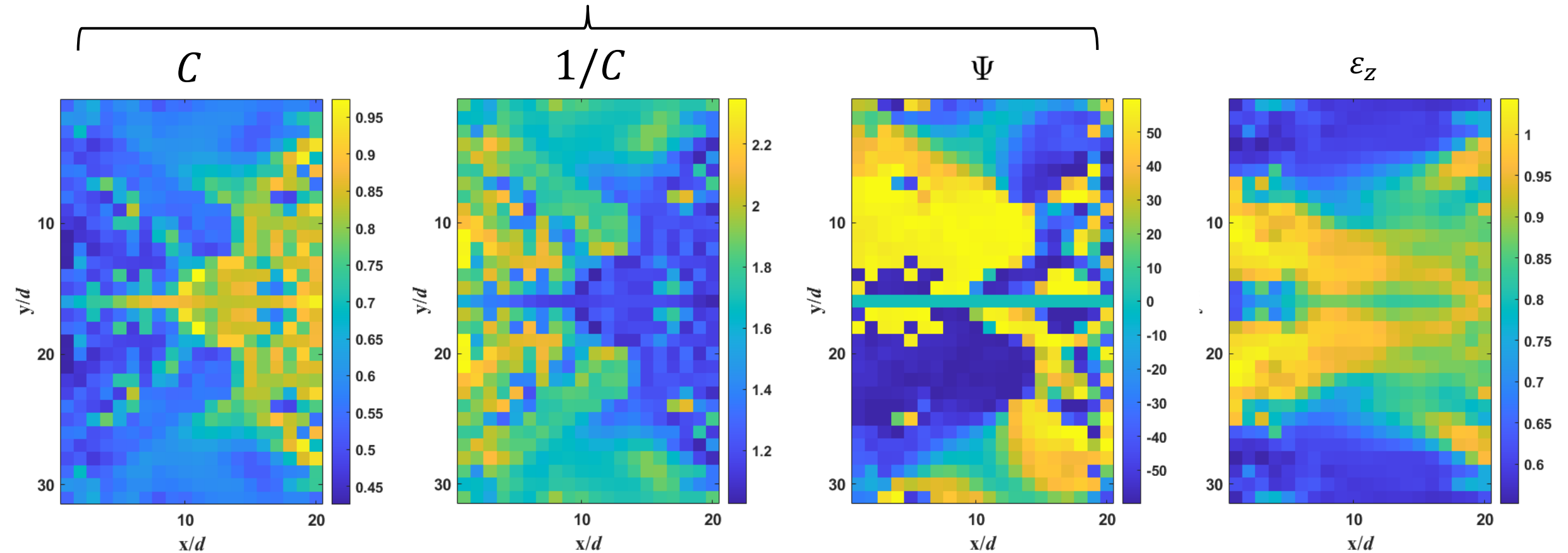
Aperture Field Profile



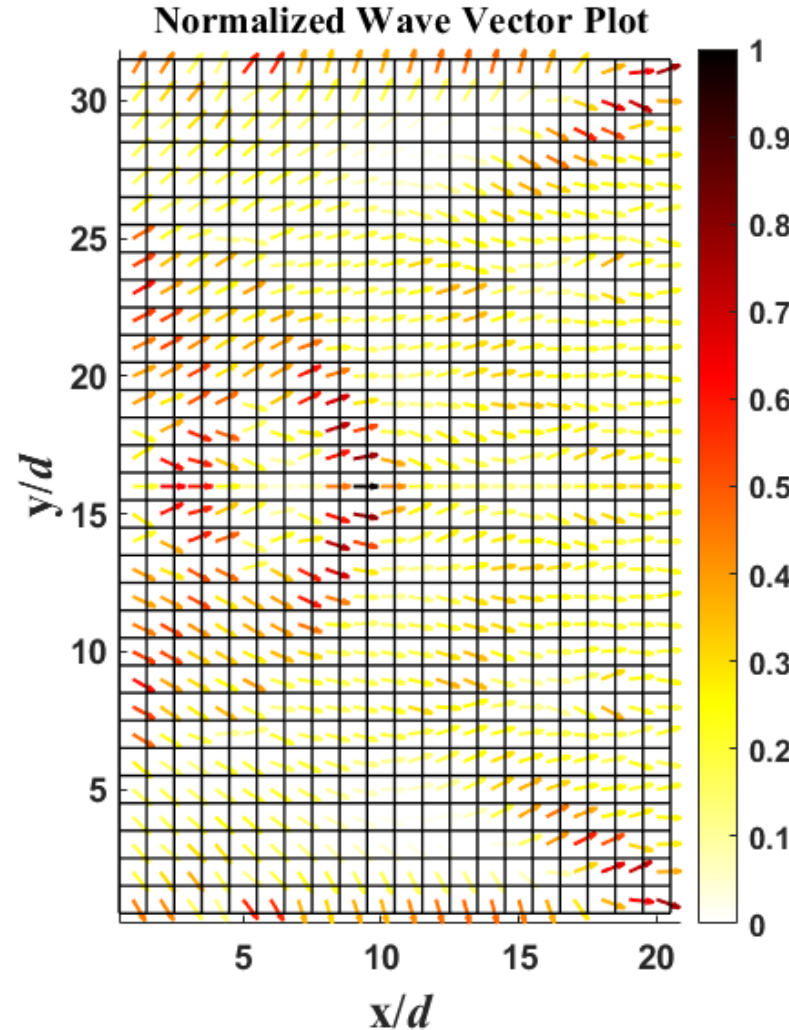
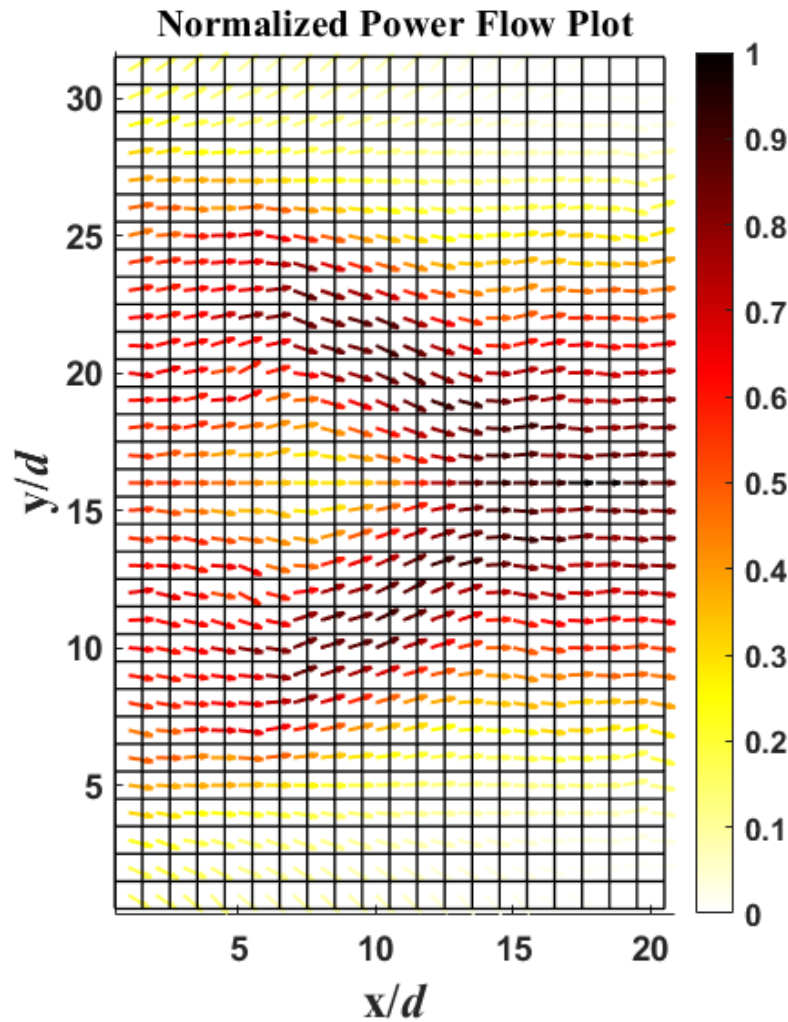
Design Specifications

Center frequency	10 GHz
Discretization	2.5mm ($\lambda_0/12$)
Collimator width	7.75 cm (31 columns)
Collimator depth	5 cm (20 columns)

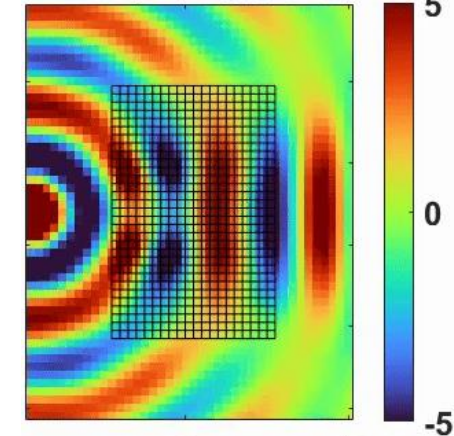
$$\bar{\mu}(x, y) = R^T(\Psi) \sqrt{\Delta} \begin{bmatrix} C & 0 \\ 0 & \frac{1}{C} \end{bmatrix} R(\Psi)$$



Control of phase progression and power flow direction

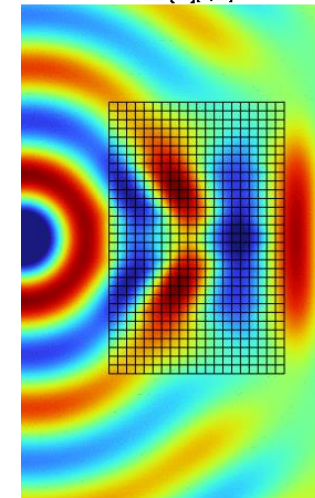


Real $\{V(x, y)\}$ [V]



Circuit
Network
Solver

Real $\{E_z\}$ [V/m]



COMSOL

Perfectly-matched metamaterial
is outlined in the black box

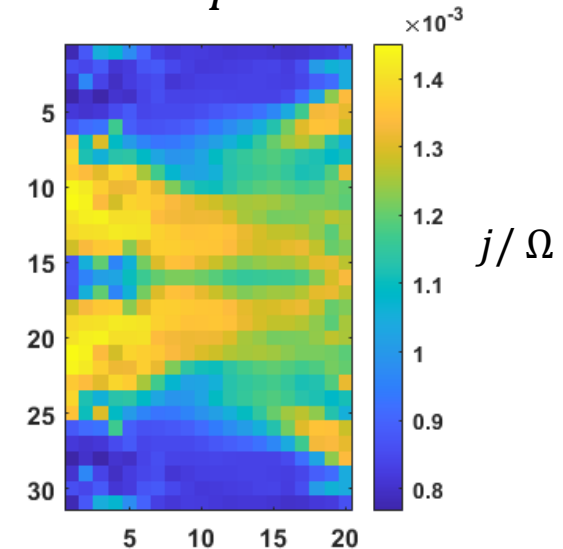
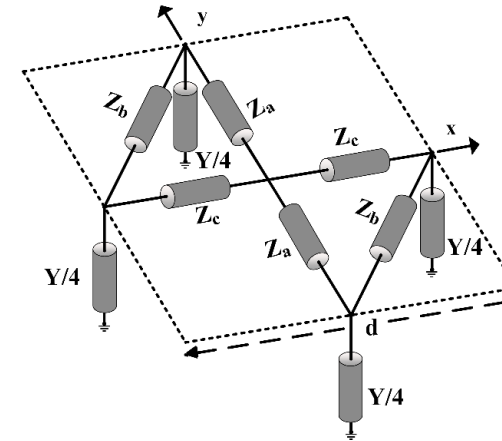
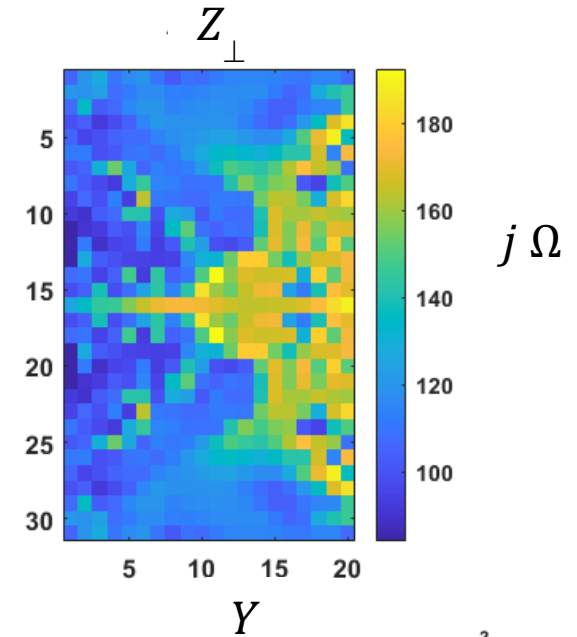
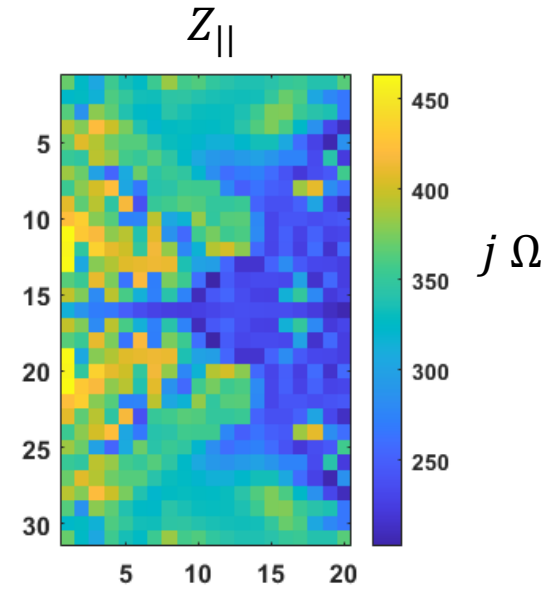
Circuit parameters of inverse designed collimator



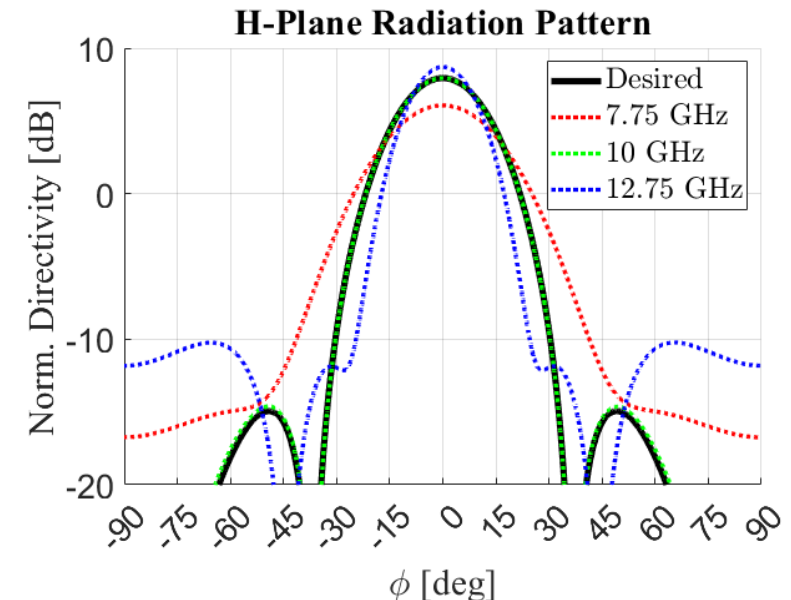
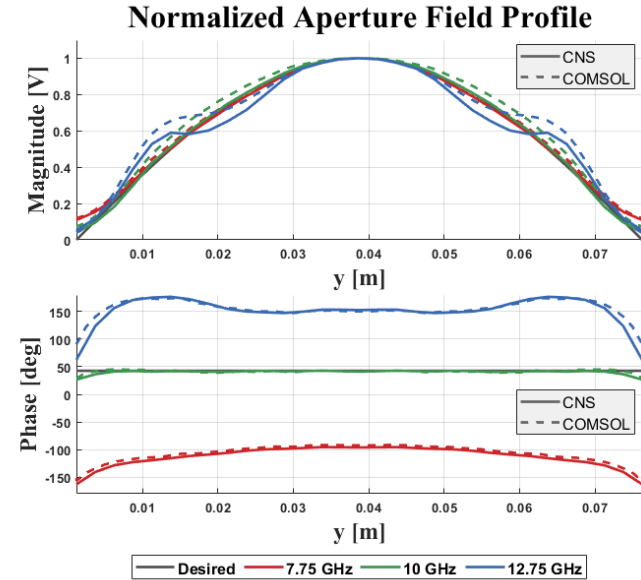
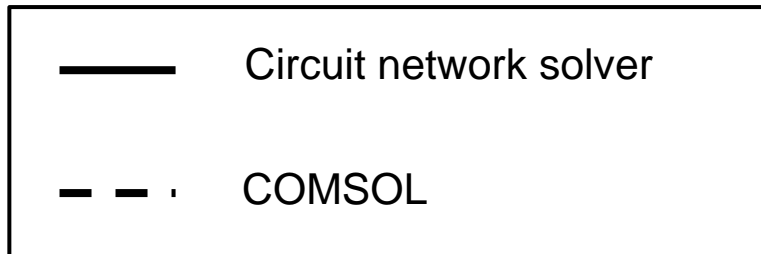
- Broadband devices must have material parameters that are non dispersive/of a low-pass topology.
- In the context of the circuit network, a low-pass topology consists of series inductive impedances and shunt capacitive impedances.
- The series impedance plots ($Z_{||}$ and Z_{\perp}) confirm that they are inductive everywhere. The shunt impedances (Y) confirm that they are capacitive everywhere

Series Impedance Tensor

$$\bar{\bar{Z}} = \begin{bmatrix} \frac{2Z_c(Z_a + Z_b)}{Z_a + Z_b + Z_c} & \frac{-2Z_a Z_c}{Z_a + Z_b + Z_c} \\ \frac{-2Z_a Z_c}{Z_a + Z_b + Z_c} & \frac{2Z_a(Z_c + Z_b)}{Z_a + Z_b + Z_c} \end{bmatrix} = \begin{bmatrix} \cos(\theta) & \sin(\theta) \\ -\sin(\theta) & \cos(\theta) \end{bmatrix} \begin{bmatrix} Z_{||} & 0 \\ 0 & Z_{\perp} \end{bmatrix} \begin{bmatrix} \cos(\theta) & -\sin(\theta) \\ \sin(\theta) & \cos(\theta) \end{bmatrix}$$



- The PMM exhibits an 50% (5 GHz) bandwidth from 7.75 GHz – 12.75 GHz.
- The PMM was optimized at a design frequency of 10 GHz, at which it collimates **88%** of the incident power.
- **Across the bandwidth of operation:**
 - The efficiency are within $\pm 5\%$
 - The sidelobe levels are within 3 dB of the desired pattern ($SLL_{des} = 22$ dB)
 - Maximum directivity is within ± 1.5 dB of the desired pattern
 - Half-power beamwidth is within $\pm 20\%$ of the desired pattern
- Comparing the Circuit Network Solver (CNS) with COMSOL we observe a good agreement across the bandwidth of the device.



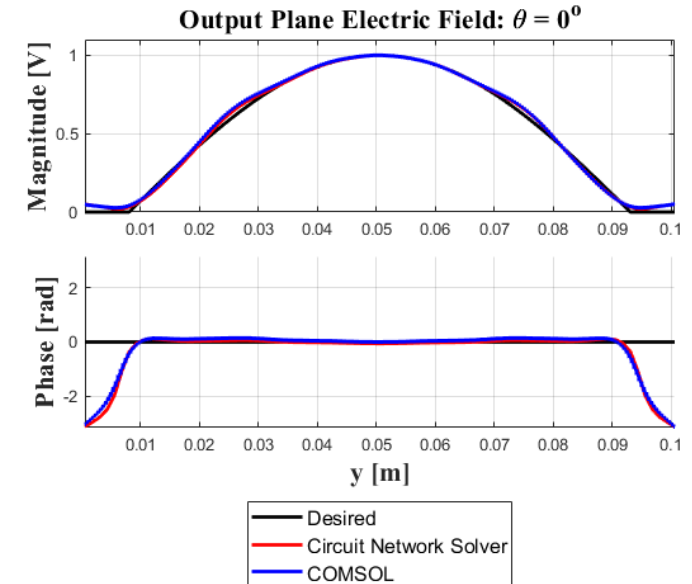
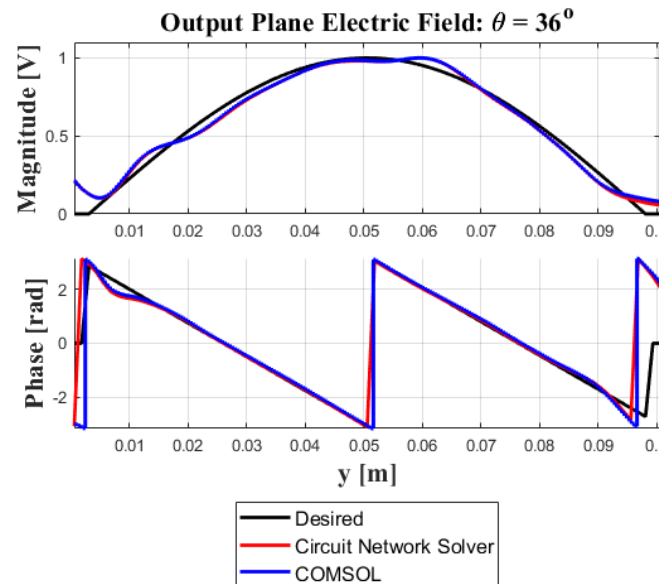
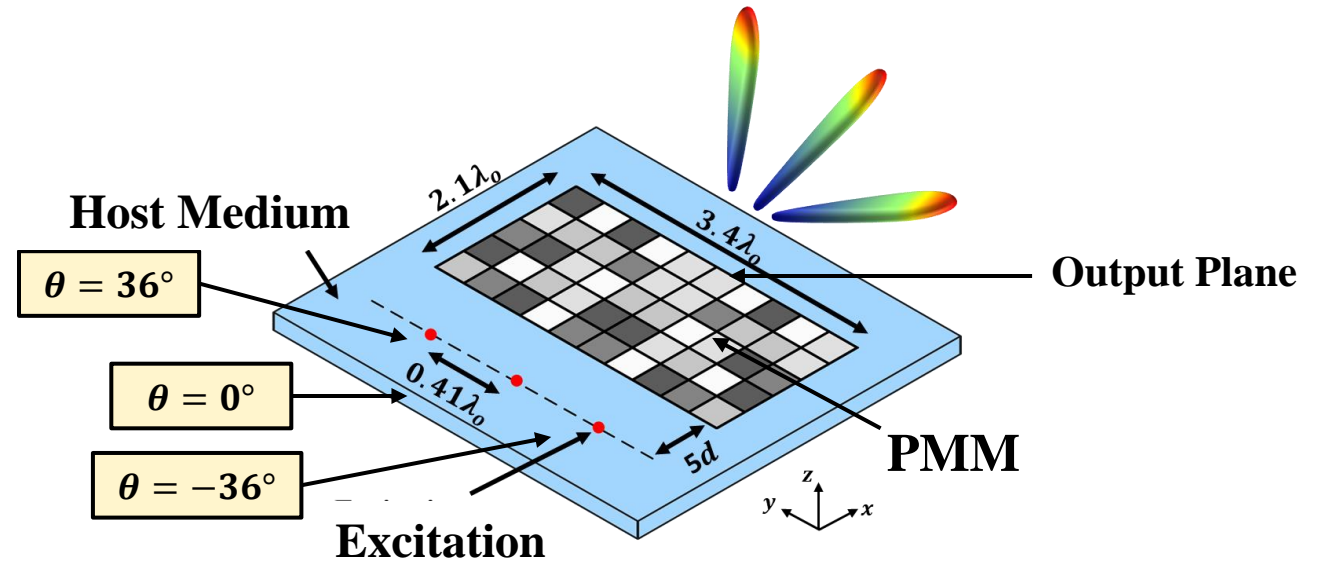
Inverse design: MIMO beamformer with zero scan loss



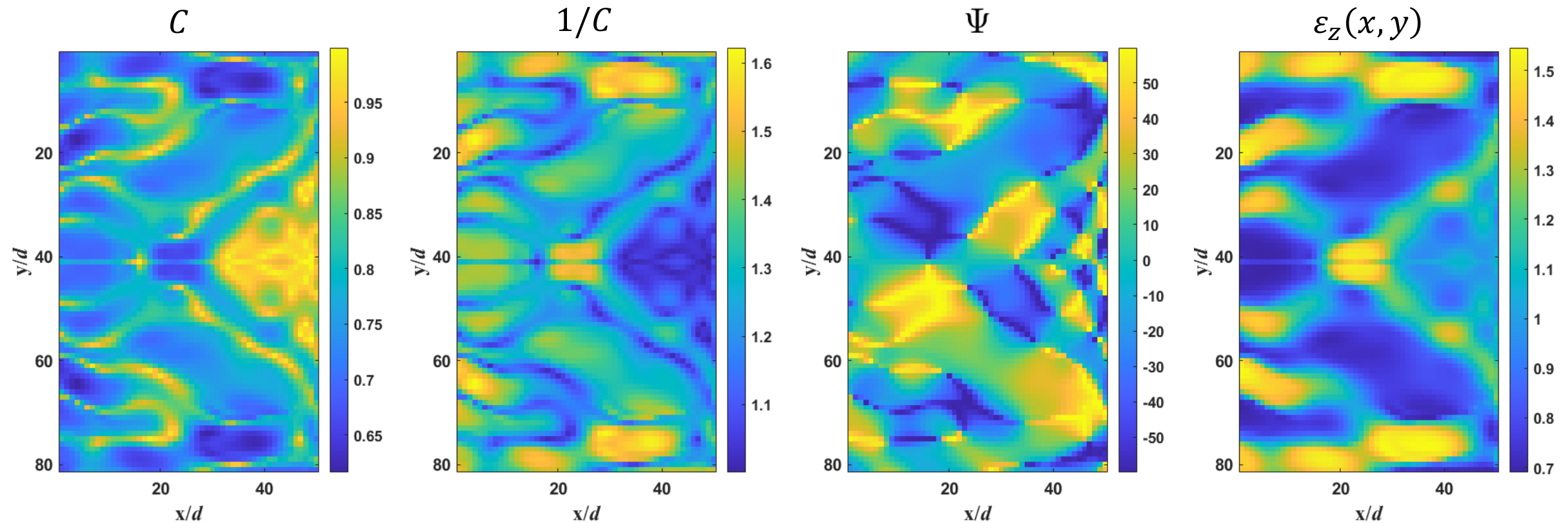
Design Specifications

Center frequency	10 GHz
Discretization	1.25 mm ($\lambda_0/24$)
Collimator width	10.1 cm (81 rows)
Collimator depth	6.25 cm (50 cols)
Radiation Angle (θ)	$\{-36^\circ, 0^\circ, 36^\circ\}$

- MIMO Zero-Scan-Loss Beamformer: A 3-Input 3-Output beamformer with identical directivities for different radiation angles
- Symmetry is imposed across the centerline due to the symmetry of the transformation



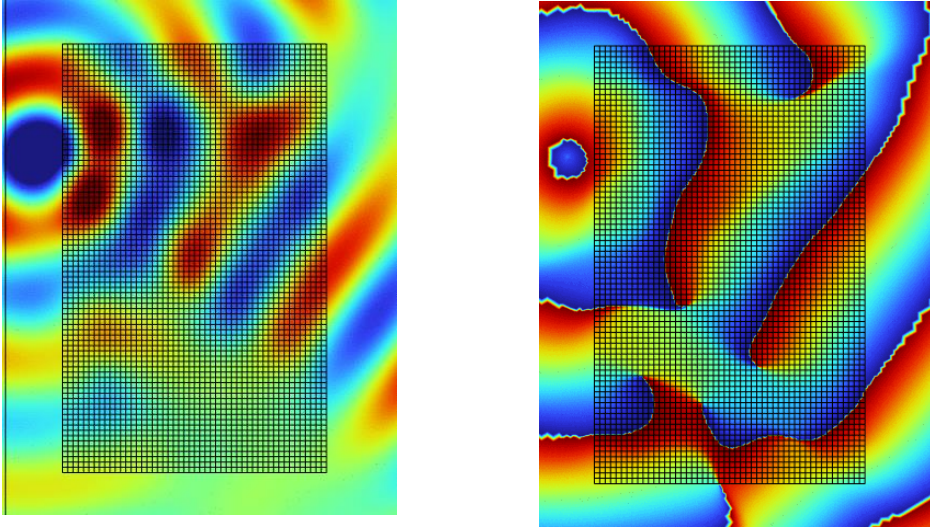
$$\bar{\bar{\mu}}(x, y) = \underbrace{\bar{\bar{R}}^T(\Psi) \begin{bmatrix} C & 0 \\ 0 & \frac{1}{C} \end{bmatrix} \bar{\bar{R}}(\Psi)}_{\text{Material parameters}}$$



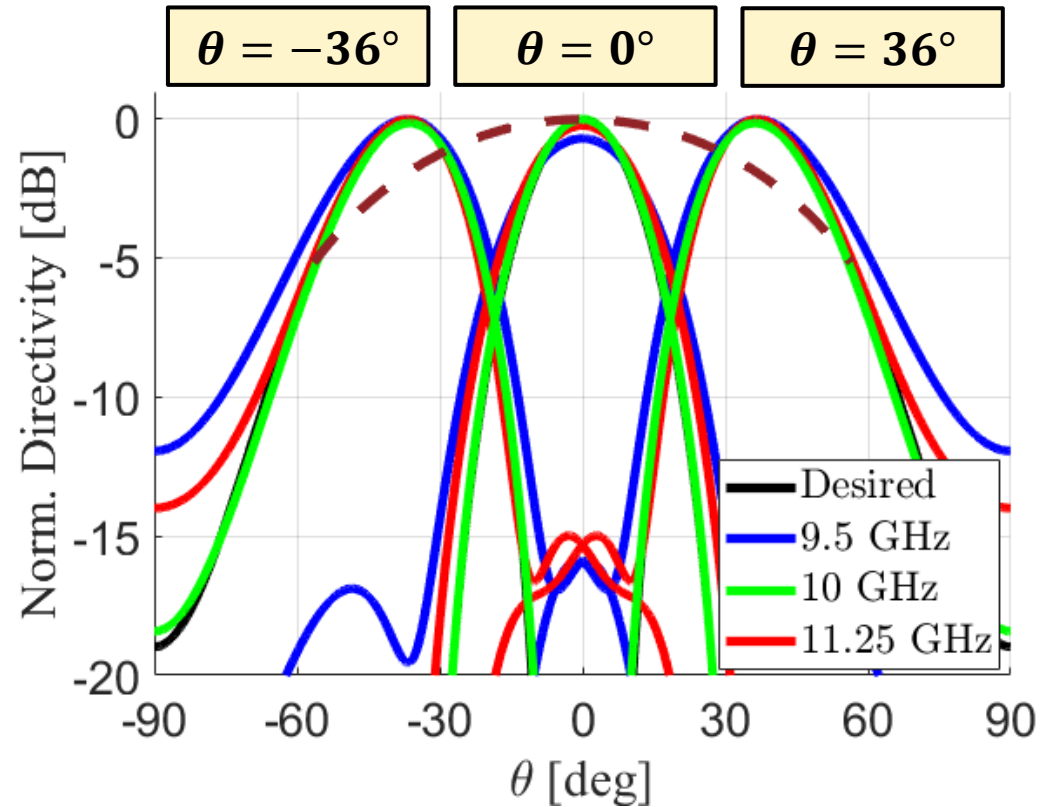
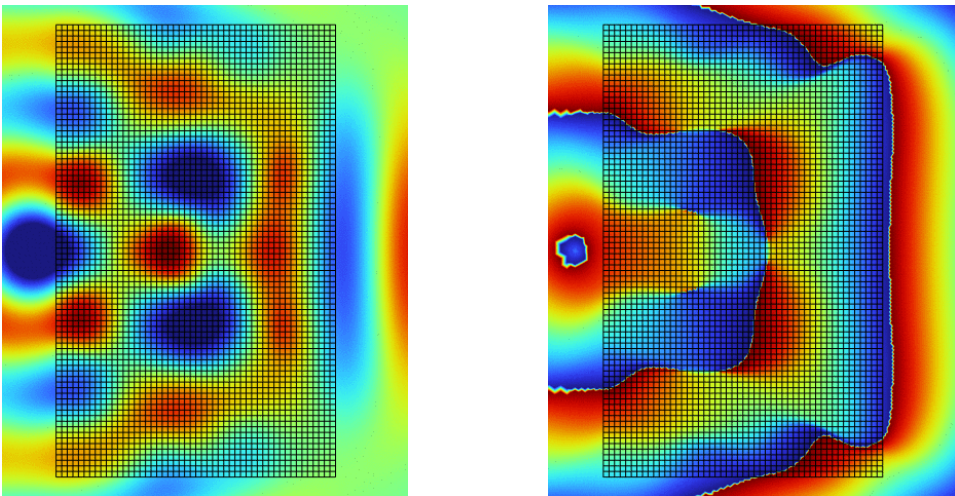
Performance of zero-scan-loss beamformer



Case1: $\theta = 36^\circ$



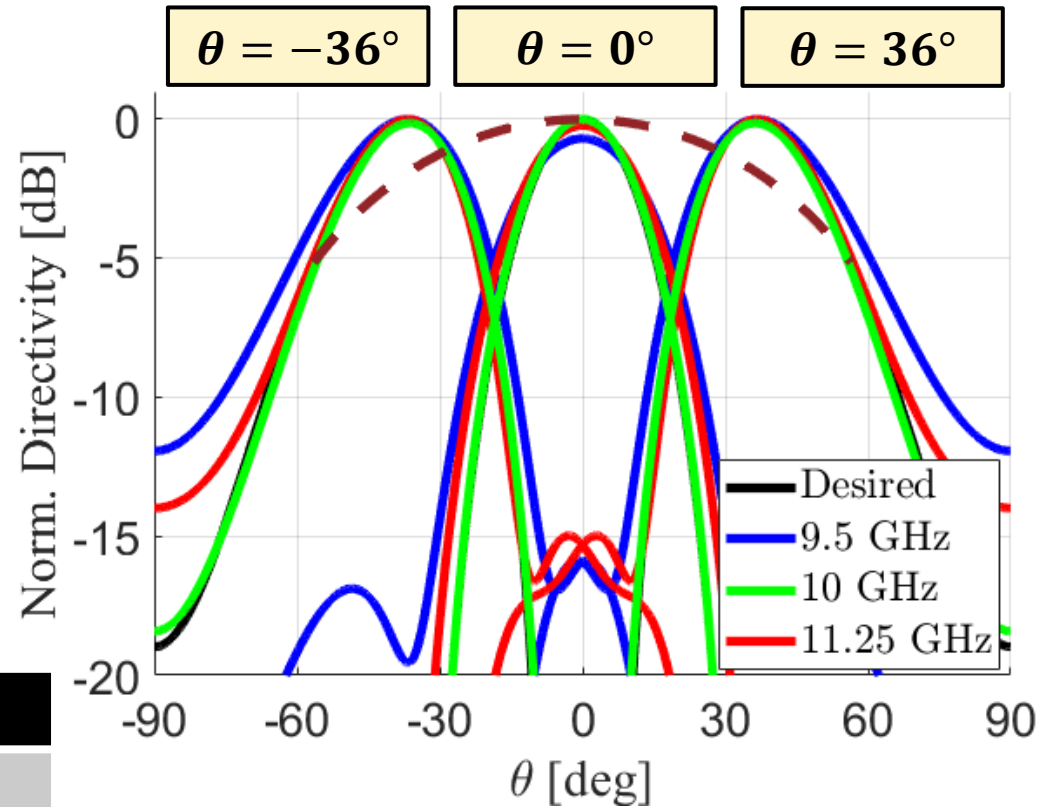
Case2: $\theta = 0^\circ$



S. Thakkar, J. Ruiz-García, L. Szymanski, G. Gok, and A. Grbic, "Inverse Design of Perfectly-Matched Metamaterials Via Circuit-Based Surrogate Models and the Adjoint Method," under review in *IEEE Trans. on Microwave Theory and Techniques*, submitted Jan. 2025.

Performance of zero-scan-loss beamformer continued

- The perfectly-matched metamaterial (PMM) has a 1.75 GHz bandwidth from 9.5 GHz – 11.25 GHz.
- The PMM was optimized at a design frequency of 10 GHz, at which it collimates 70% of the incident power.
- Across the bandwidth of operation:
 - The sidelobe levels are better than 15 dB
 - Scan loss experienced is less than 0.5 dB
- Circuit Network Solver (CNS) and COMSOL show good agreement across the bandwidth of the device.



Frequency	Scan Loss
Expected Scan Loss (brown)	1.9 dB
9.5 GHz	0.5 dB
10 GHz	0.15 dB
11.25 GHz	0.3 dB

- Introduced the concept of Perfectly-Matched Metamaterials (PMMs)
 - Constitutive unit cells are impedance matched to each other and surrounding medium.
- Showed that PMMs locally control the phase progression and power flow.
 - Closed-form expressions for the material parameters (ε_z and $\bar{\mu}$) in terms of wave vector and power flow direction were derived.
- PMMs enable reflectionless multiple-input multiple-output field transformations.
- Analytic design procedure was reported for single-input single-output devices.
- Inverse design strategy proposed for multiple-input multiple-output devices.
- Next step: fabrication and experimental verification of devices.

Applications: antenna beamformers, MIMO antennas, analog computation, neural network design.

- [1] S. Thakkar, J. Ruiz-García, L. Szymanski, G. Gok, and A. Grbic, "Beamforming with Perfectly-Matched Metamaterials," *2025 19th European Conference on Antennas and Propagation (EuCAP)*, accepted, Stockholm, Sweden, submitted Sep.2024.
- [2] S. Thakkar, J. Ruiz-García, L. Szymanski, G. Gok, and A. Grbic, "Inverse Design of Perfectly-Matched Metamaterials Via Circuit-Based Surrogate Models and the Adjoint Method," under review in *IEEE Trans. Microwave Theory and Techniques.*, submitted Jan. 2025